THE 2012 SUMATRA GREAT EARTHQUAKE SEQUENCE

Zacharie Duputel[1], Hiroo Kanamori[1], Victor Tsai[1], Luis Rivera[2],
Lingsen Meng[1], Jean-Paul Ampuero[1] and Joann Stock[1]

1) Seismological Laboratory, California Institute of Technology
2) IPGS-EOST, Université de Strasbourg

Earthquake source physics on various scales
ECGS WORKSHOP 2012
October 3, 2012

The 2012 off-Sumatra earthquake sequence

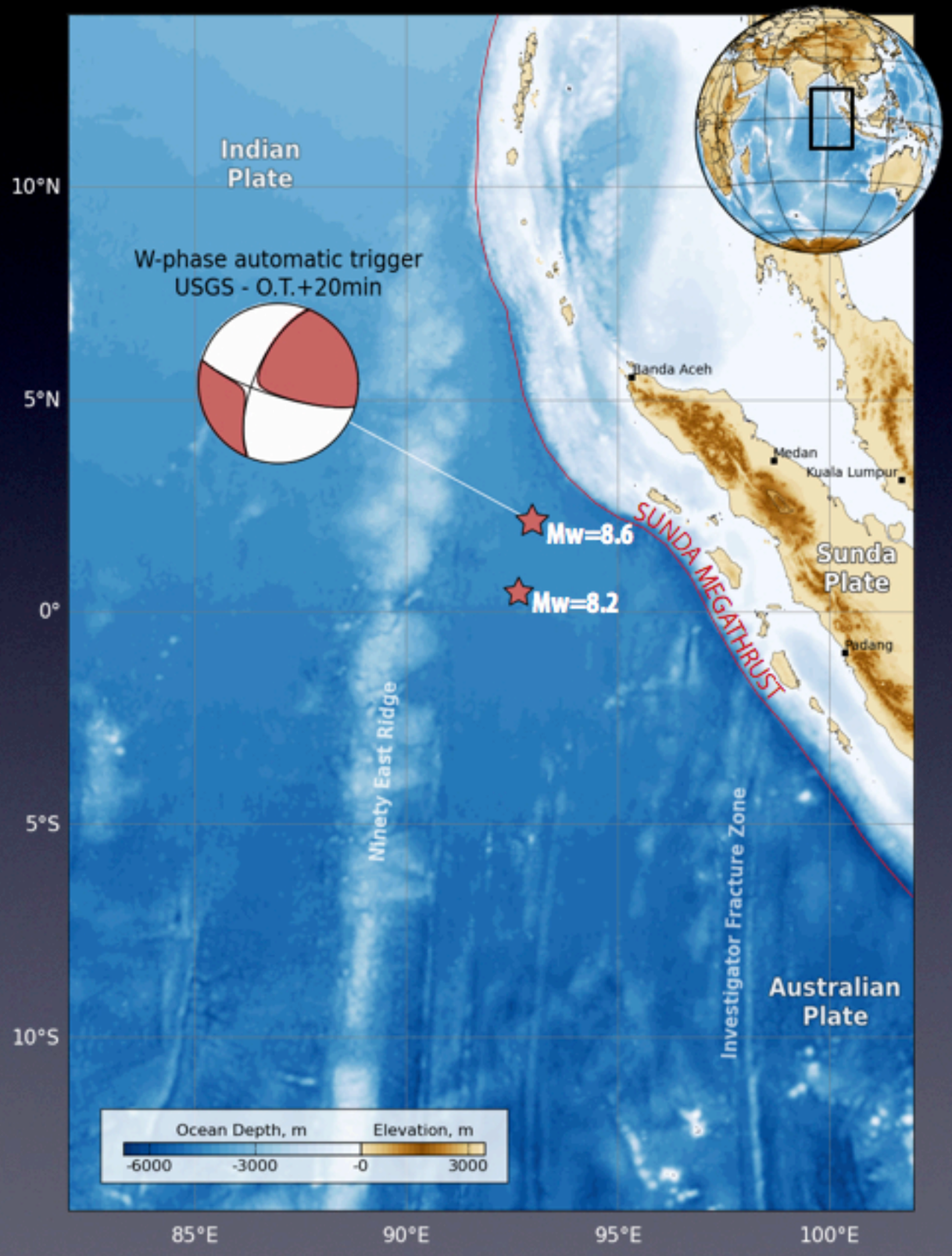

Origin Time (O.T.): 11 April 2012 - 08:39 UTC

O.T. : ***Mainshock Mw=8.6***

5min : PTWC announce M8.8 and mention the possibility of a destructive tsunami.

20min : W phase solution Mw=8.6
Strike-slip mechanism

35min : NEIC update to M8.7

1h05min : PTWC updates to M8.7

1h10min : ***Small tsunami hits Indonesia, h=30cm***

2h04min : ***Strong aftershock Mw=8.2***

The 2012 off-Sumatra earthquake sequence

Unique seismotectonic environment (equatorial Indian Ocean)

- Diffuse deformation zone separating Indian and Australian plates

"Record books" earthquake

- Largest strike-slip earthquake ever recorded
- Largest intraplate earthquake ever recorded

Rupture complexity

- Complexity of short-period body-wave waveforms
- Intricate distribution of aftershocks

Lack of geodetic data

- Goal: Provide a reliable description of the first-order source attributes using long-period (100-500s) and very long-period (~500s) data.

Outline

1. W phase point source solutions
   - Mw8.6 Mainshock
   - Mw8.2 Aftershock (O.T.+2h)
   - Smaller aftershocks (5.8≤Mw<7.0)
2. Rupture directivity
   - Radiation pattern
   - Amplitude ratios
   - Surface-wave moment rate functions
3. Multiple point-source analysis
   - Inversion result
   - Comparison with other studies
   - Centroid depth

I. Point source inversion - W phase

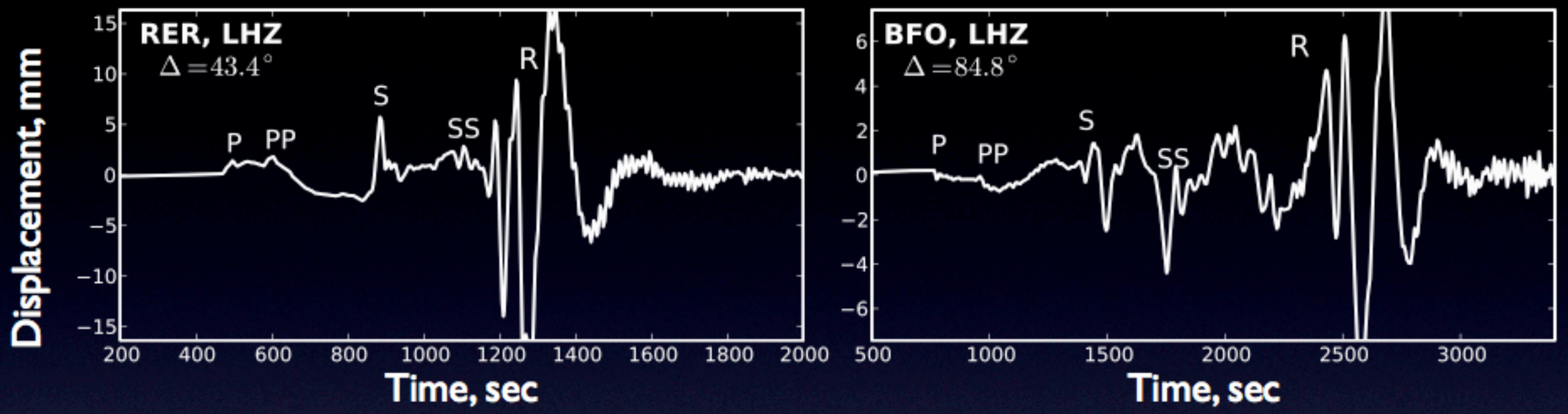

Data selection:

- 3 component velocimetric data ($\Delta \leq 90°$)
  - mainly II, IU, G, GE networks
- Based on the VLP pre-event noise (3h)

W phase:

- Full elastic field (Near + Far field)
- Group velocity: 4.5-9km/s
- Very long period (100 s - 1000 s)

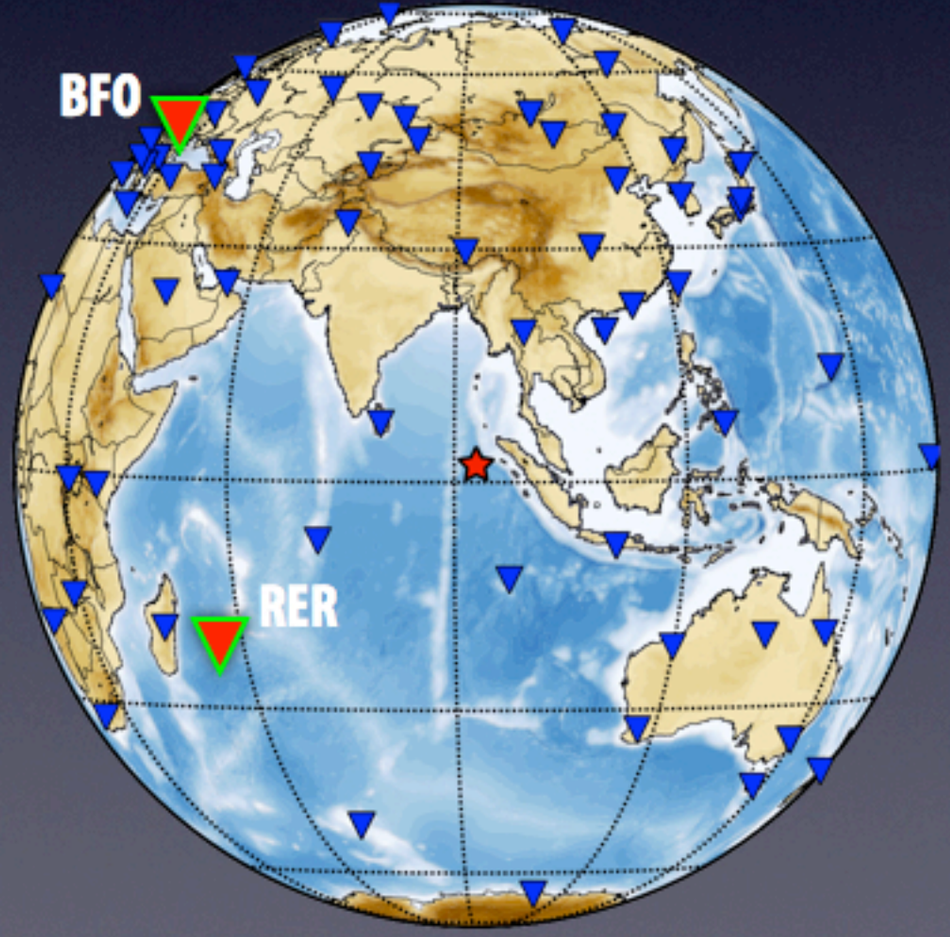

I. Point source inversion - W phase

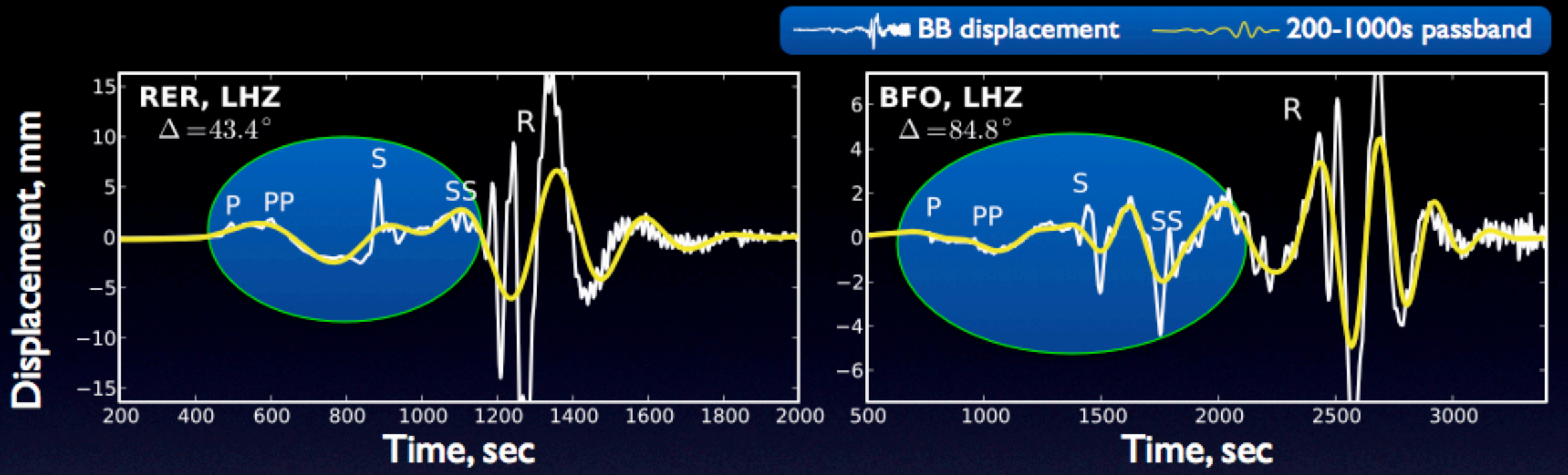

Data selection:

- 3 component velocimetric data ($\Delta \leq 90°$)
  - mainly II, IU, G, GE networks
- Based on the VLP pre-event noise (3h)

W phase:

- Full elastic field (Near + Far field)
- Group velocity: 4.5-9km/s
- Very long period (100 s - 1000 s)

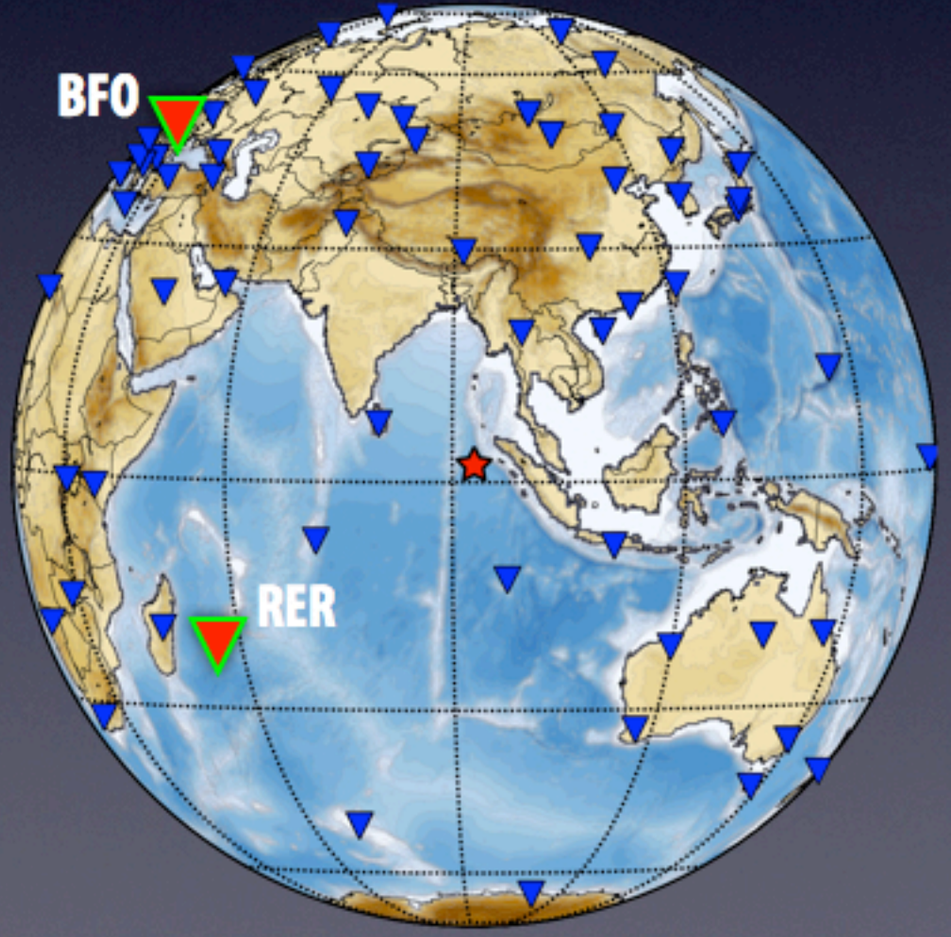

I. Point source inversion - Mw=8.6 Mainshock

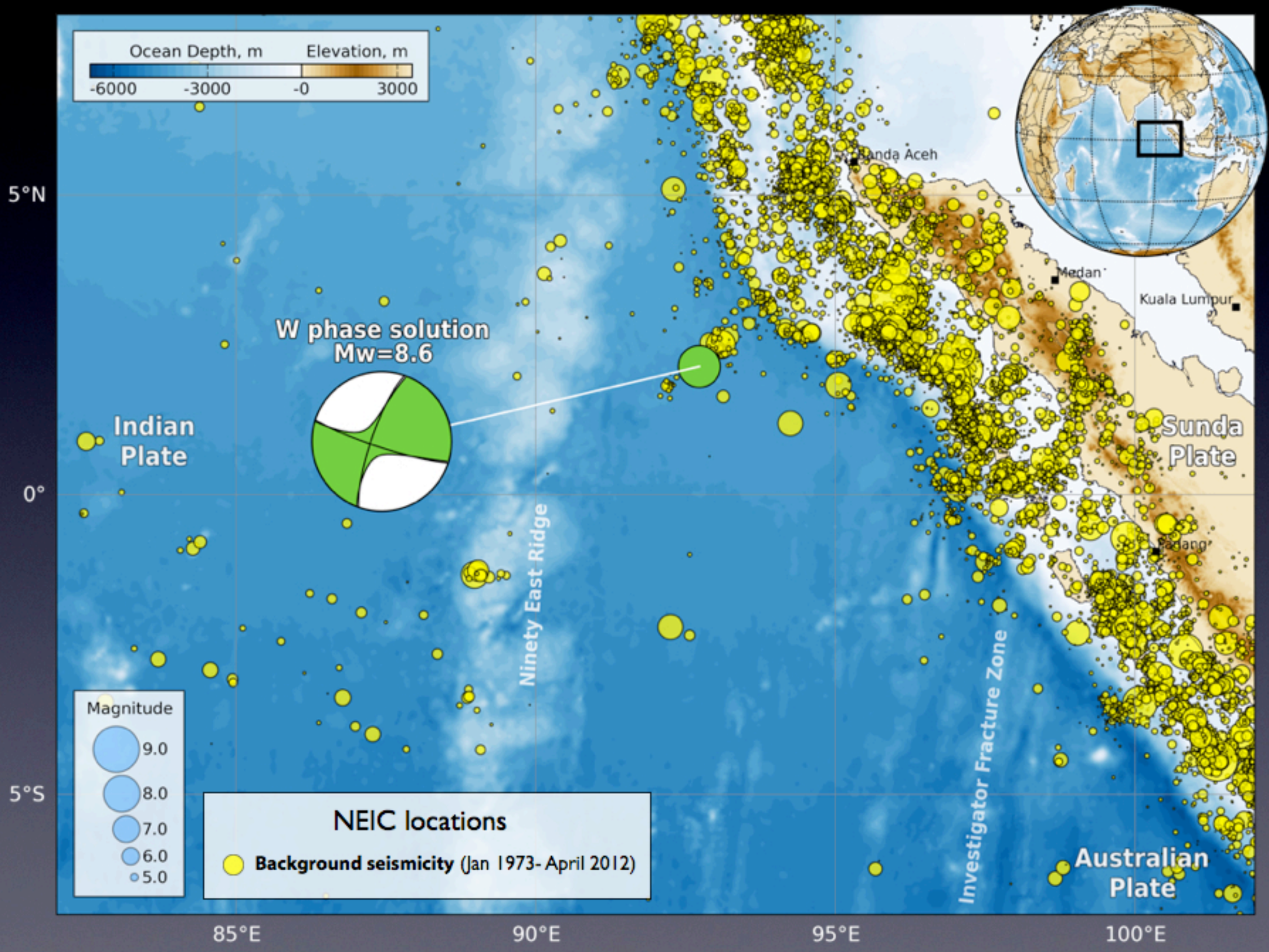

I. Point source inversion - Mw=8.6 Mainshock

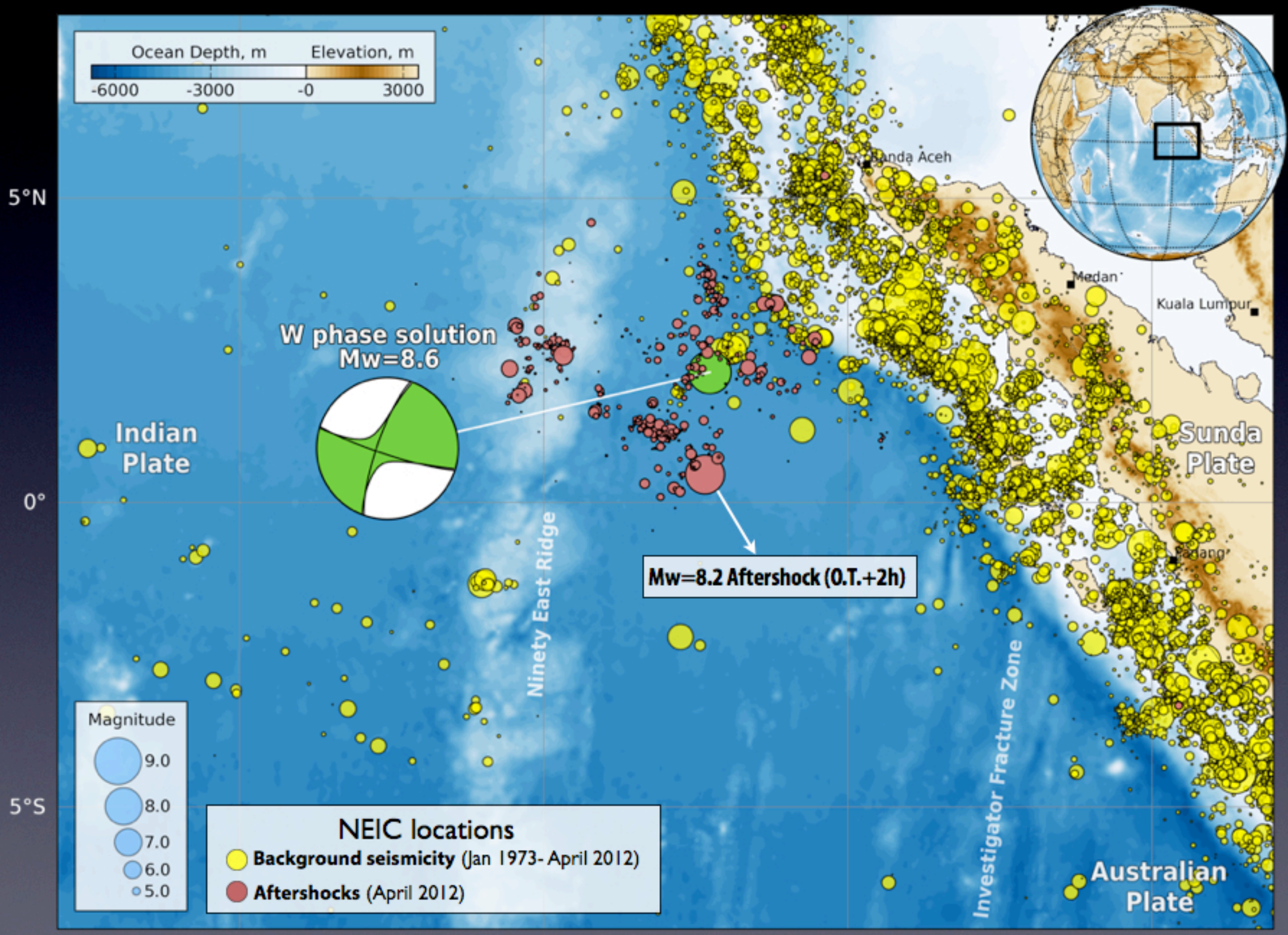

I. Point source inversion - Mw=8.2 Aftershock

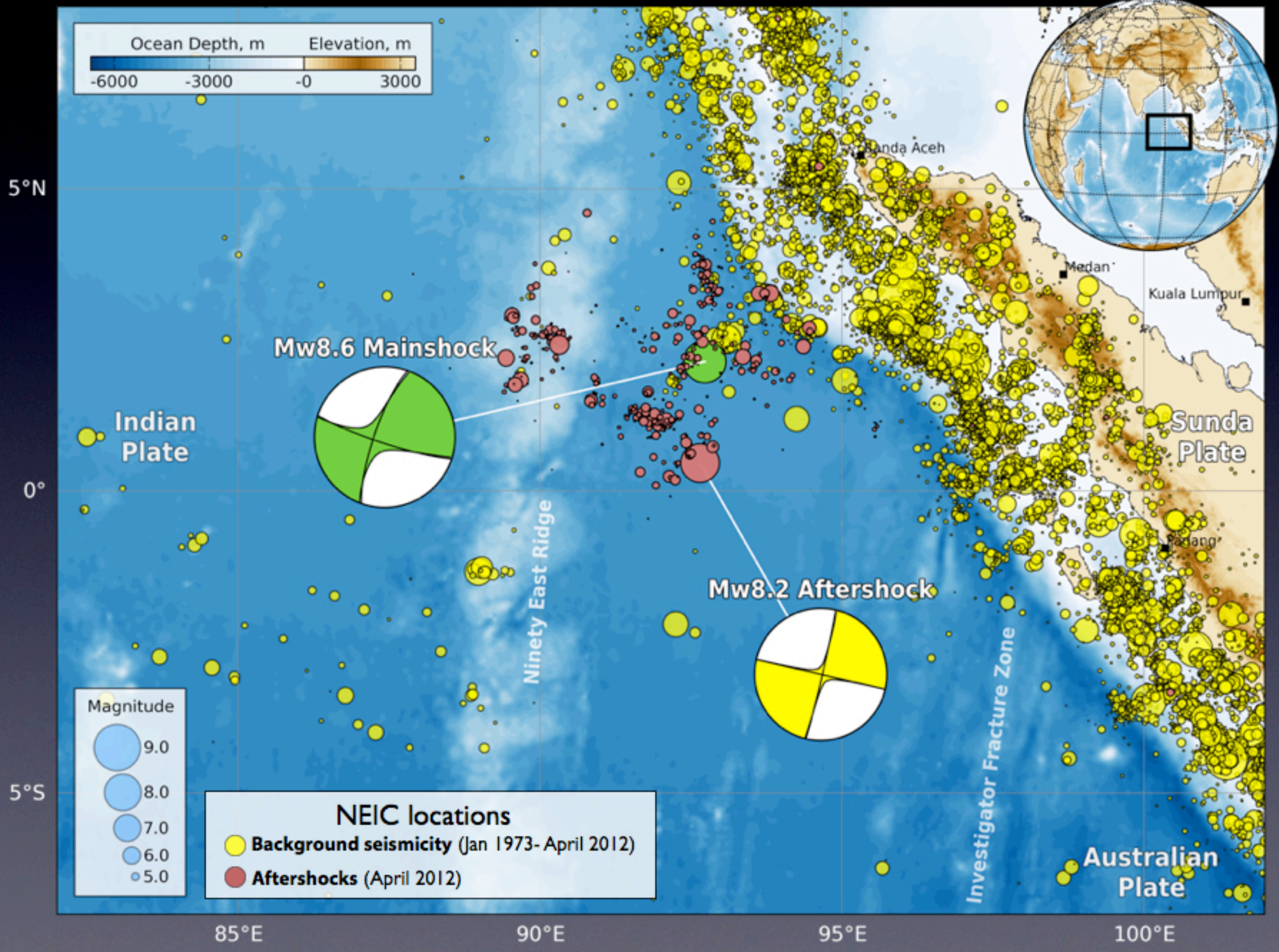

I. Point source inversion - 5.8≤Mw<8.2 Aftershocks

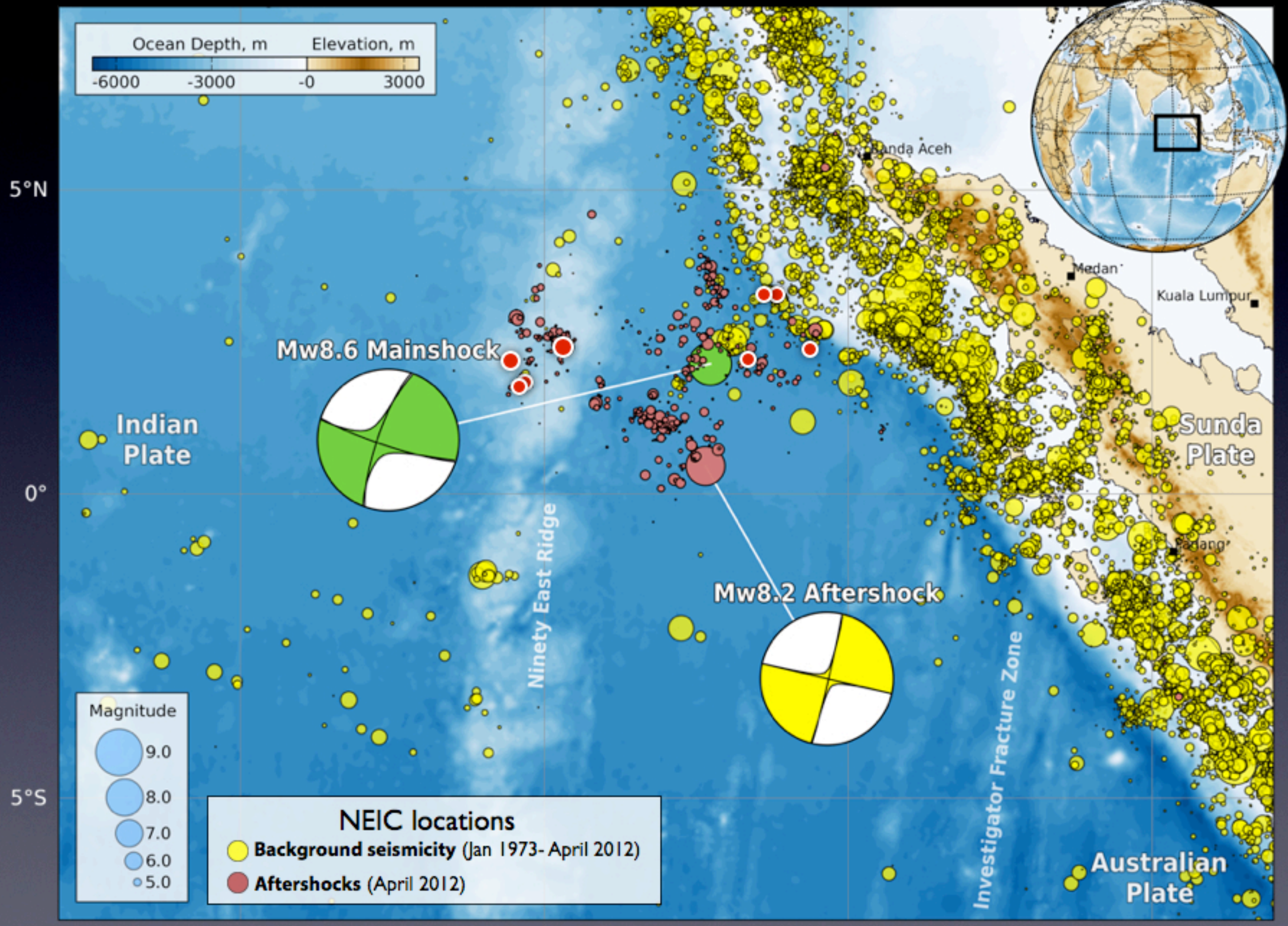

I. Point source inversion - 5.8≤Mw<8.2 Aftershocks

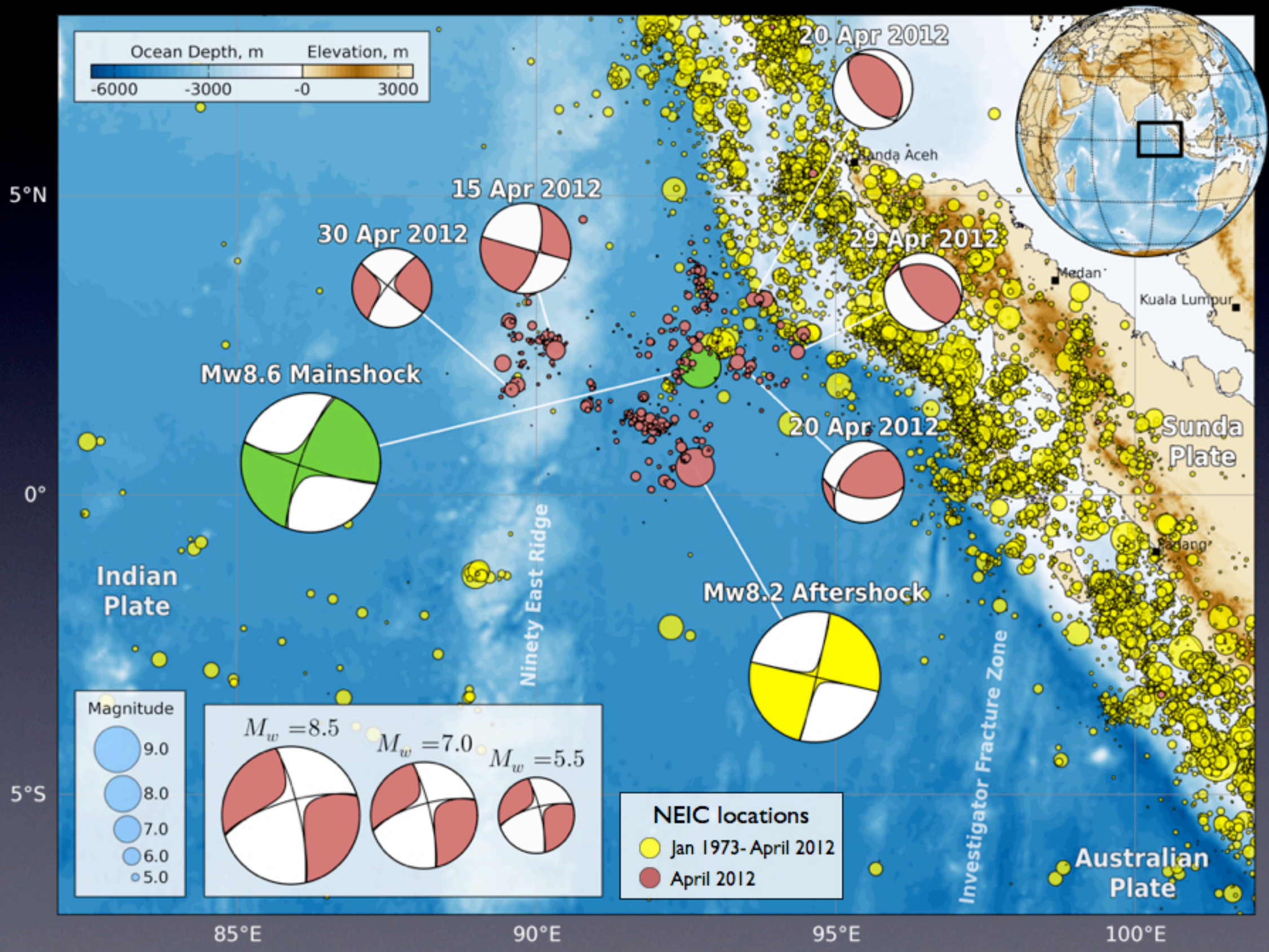

I. Point source solutions

Focal mechanisms:

- Typical for this region

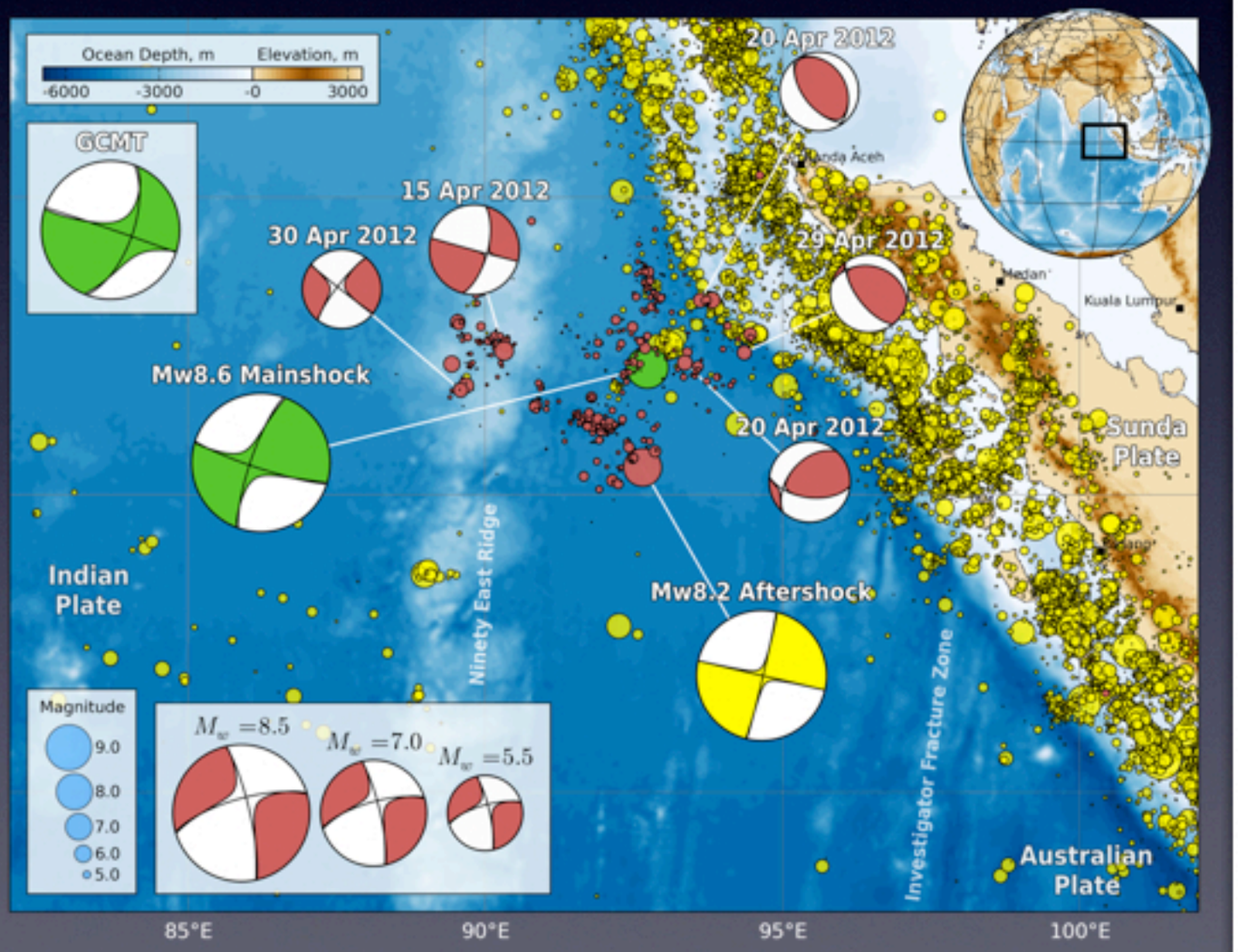

Global CMT solutions, epicenter locations from Engdahl et al., 2007

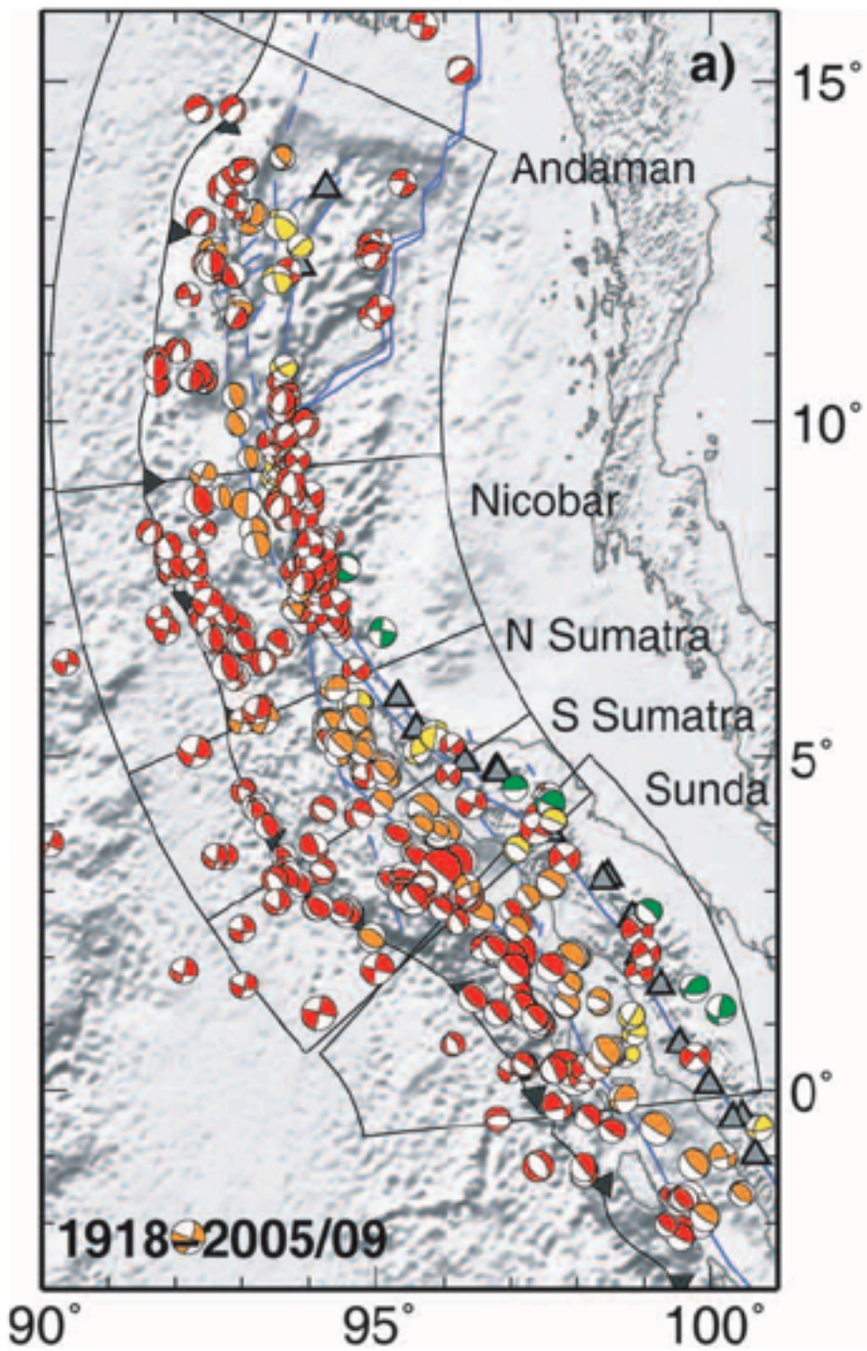

I. Point source solutions

Focal mechanisms:

- Typical for this region
- Consistent with regional strain rates

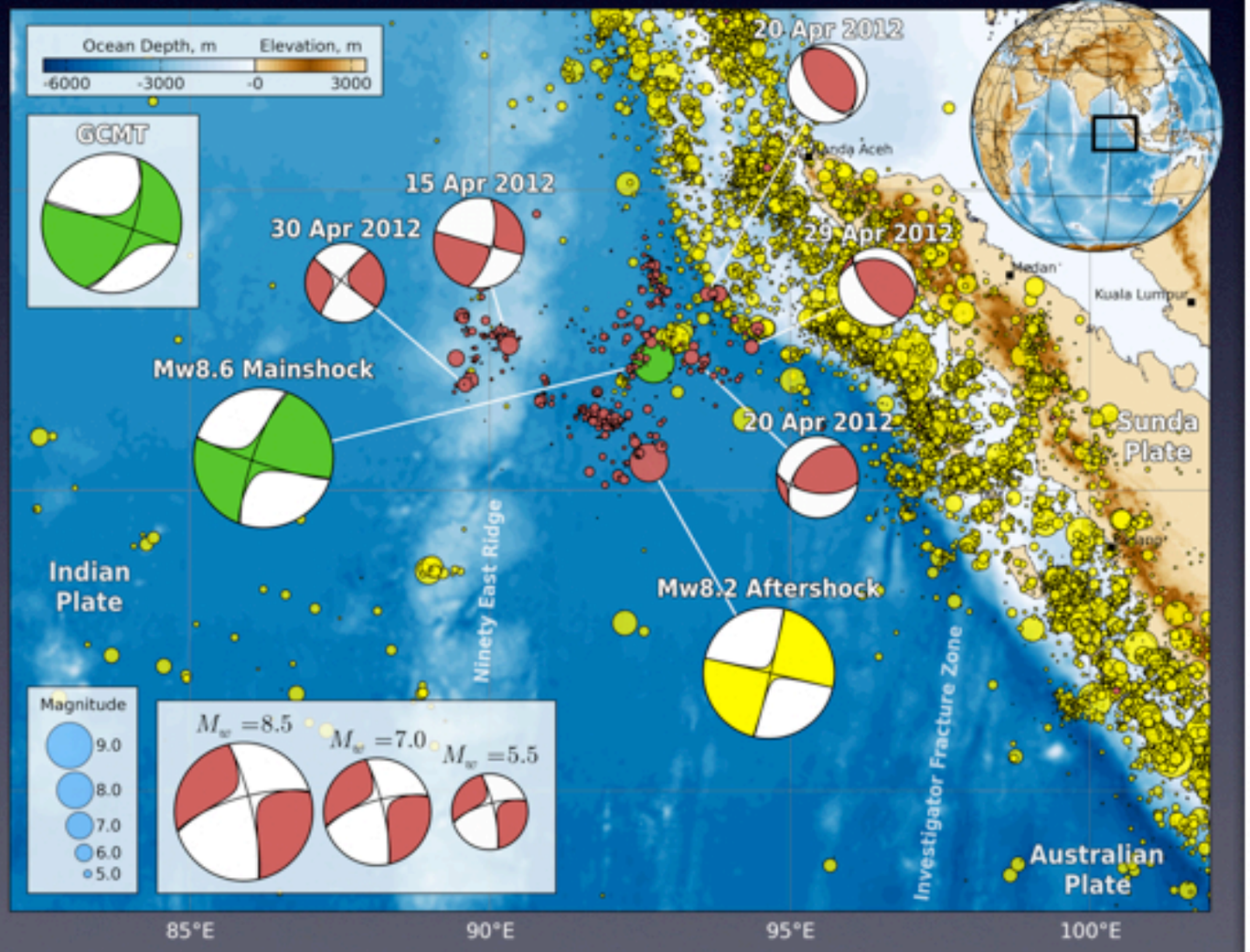

Strain-rate field modeled by
Delescluse and Chamot-Rooke (2007)

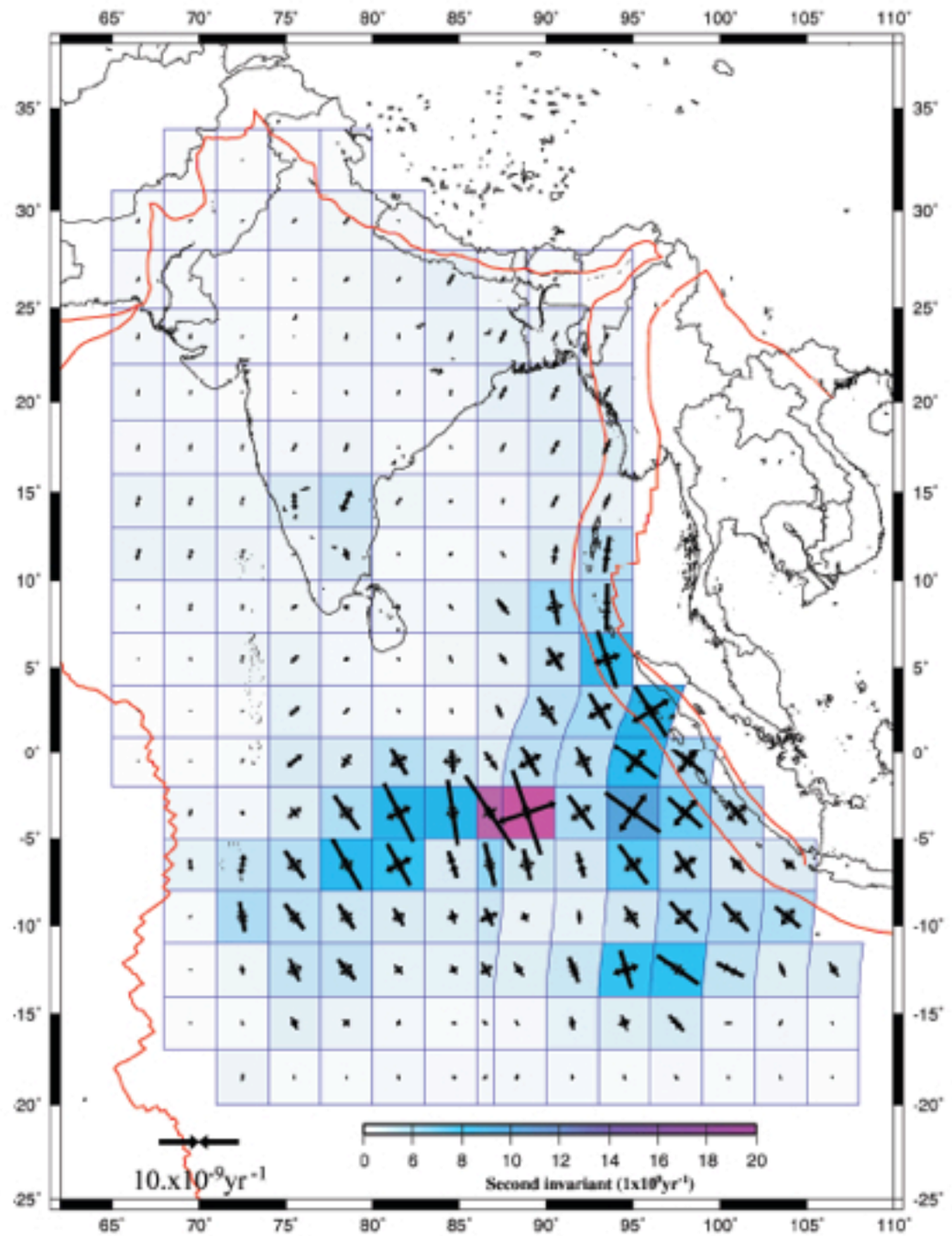

II. Surface-wave directivity for the Mw8.6 mainshock

Observed/Predicted rms amplitude ratios:

- Observed amplitudes : Short-arc (R1,G1) and long arc (R2,G2) surface waves
- Predicted amplitudes : Point source synthetics for a 3D Earth (SEM, S362ANI+Crust2.0)

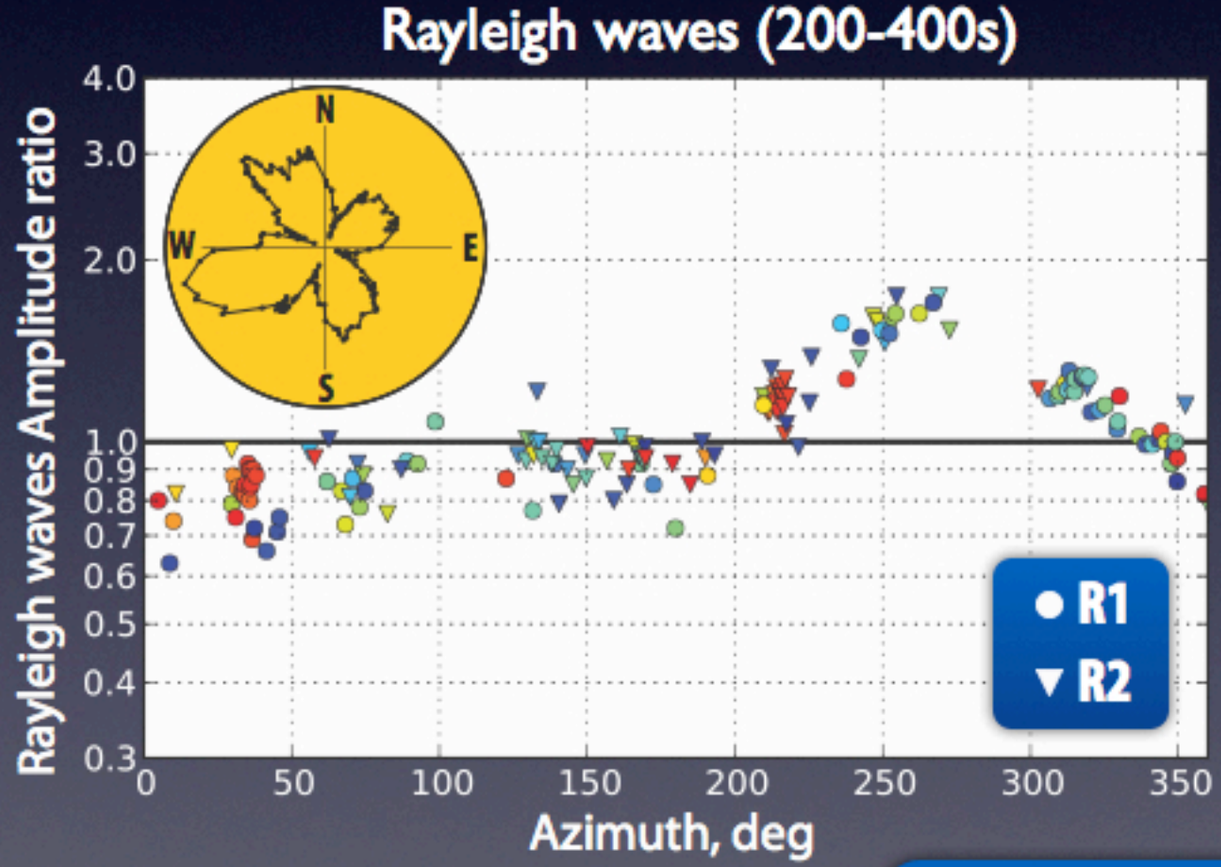

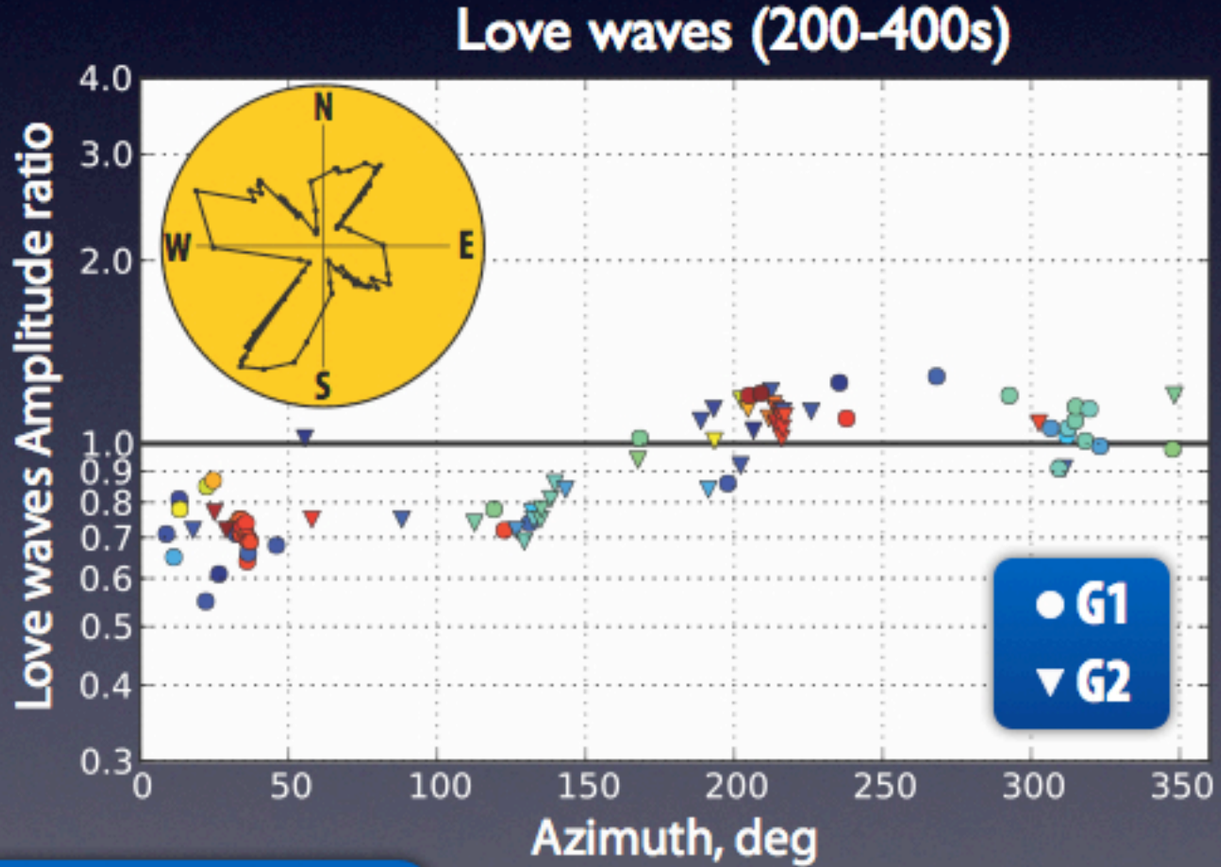

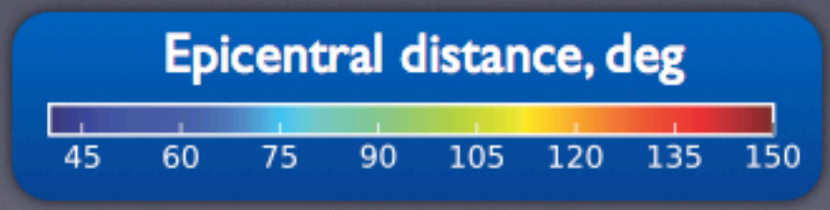

II. Surface-wave directivity for the Mw8.6 mainshock

If there were effect of finiteness, the observed/predicted amplitude would be unity for all azimuths

Rayleigh- and Love-wave amplitudes are enhanced in azimuths around 260°N (i.e., 260° clockwise from north).

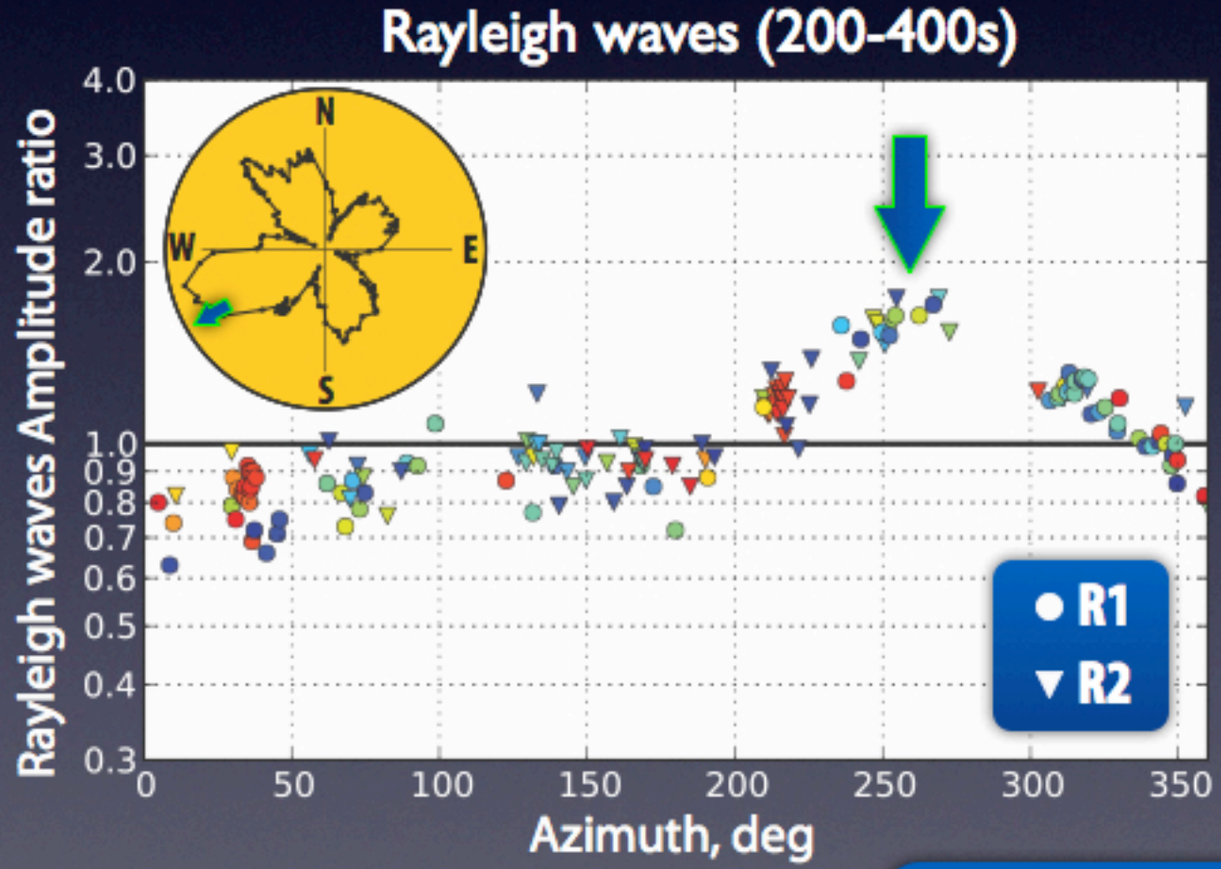

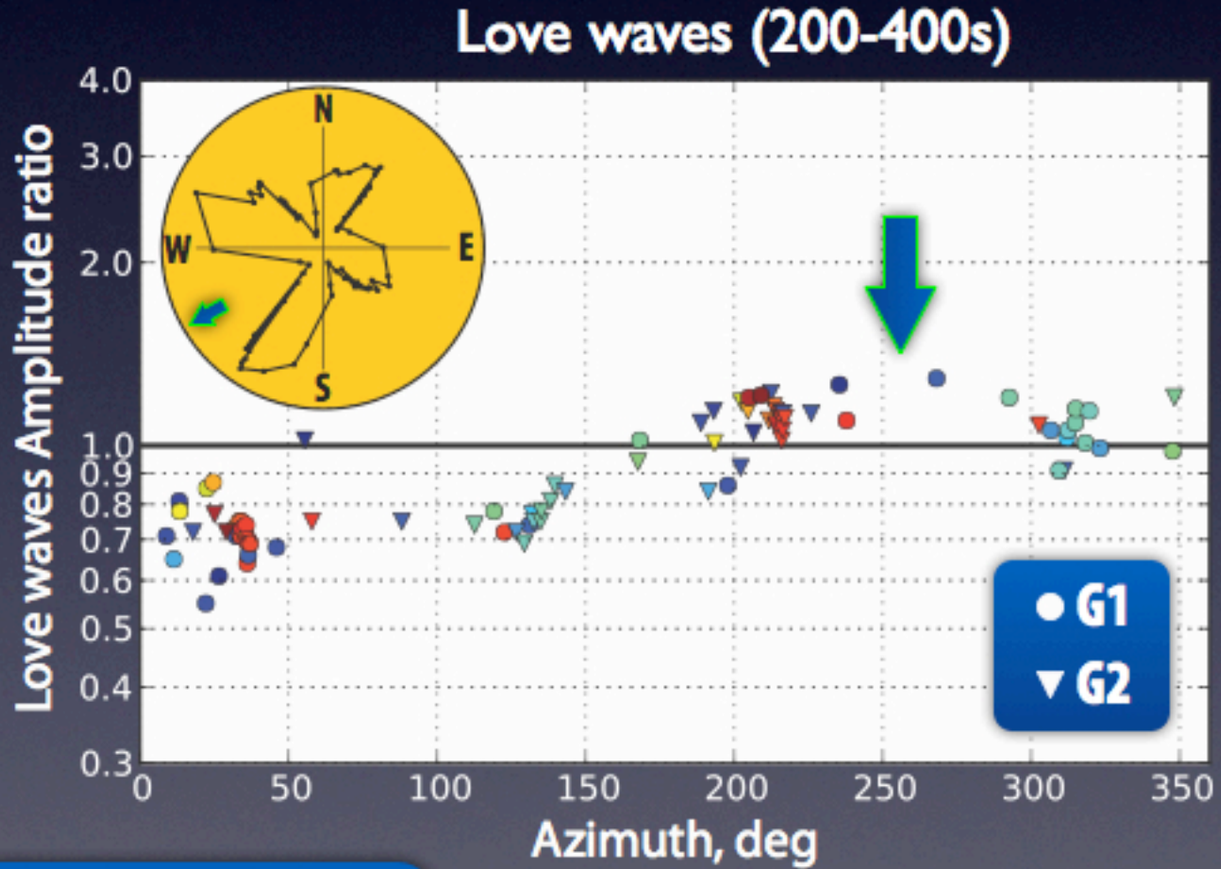

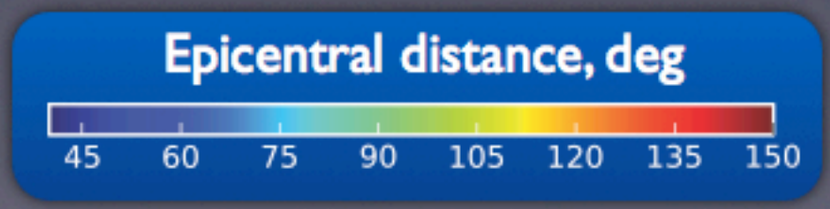

II. Surface-wave directivity for the Mw8.6 mainshock

If there were effect of finiteness, the observed/predicted amplitude would be unity for all azimuths

→ Rayleigh- and Love-wave amplitudes are enhanced in azimuths around 260°N (i.e., 260° clockwise from north).

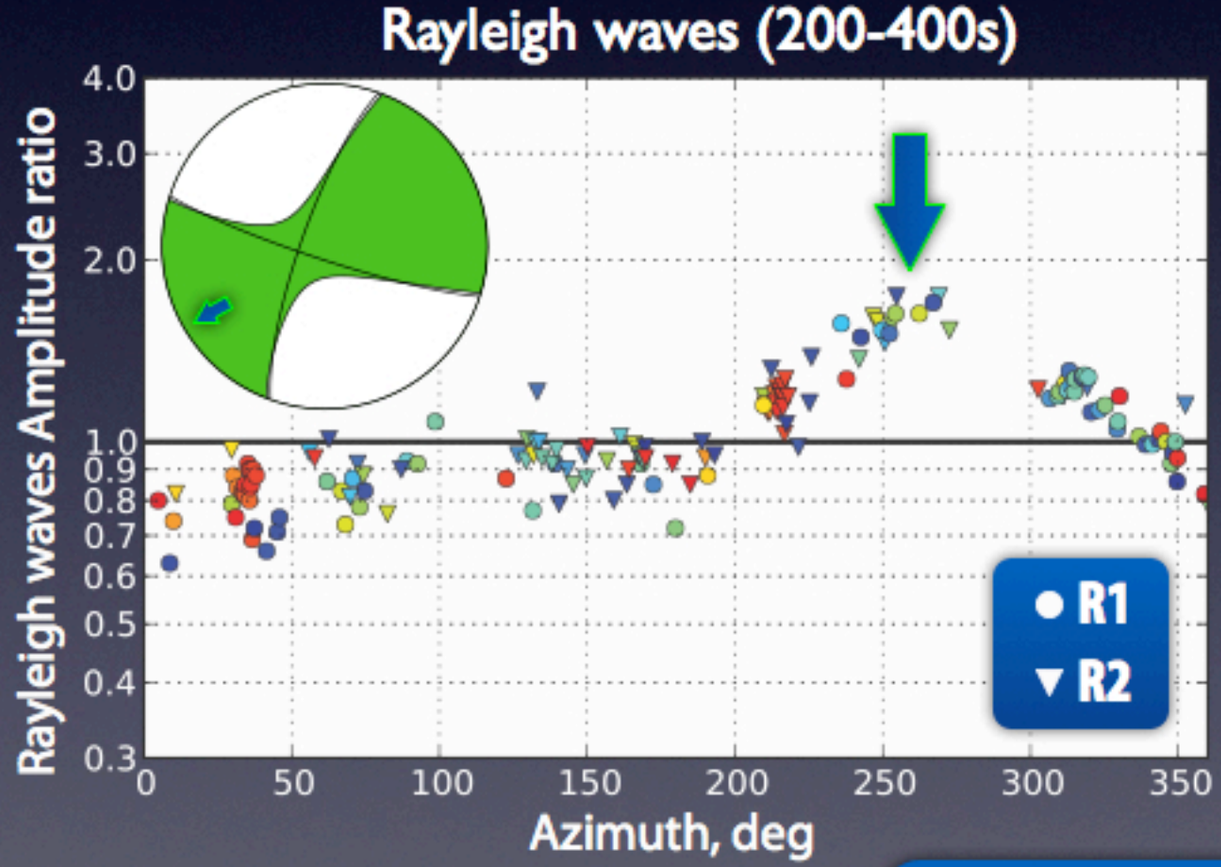

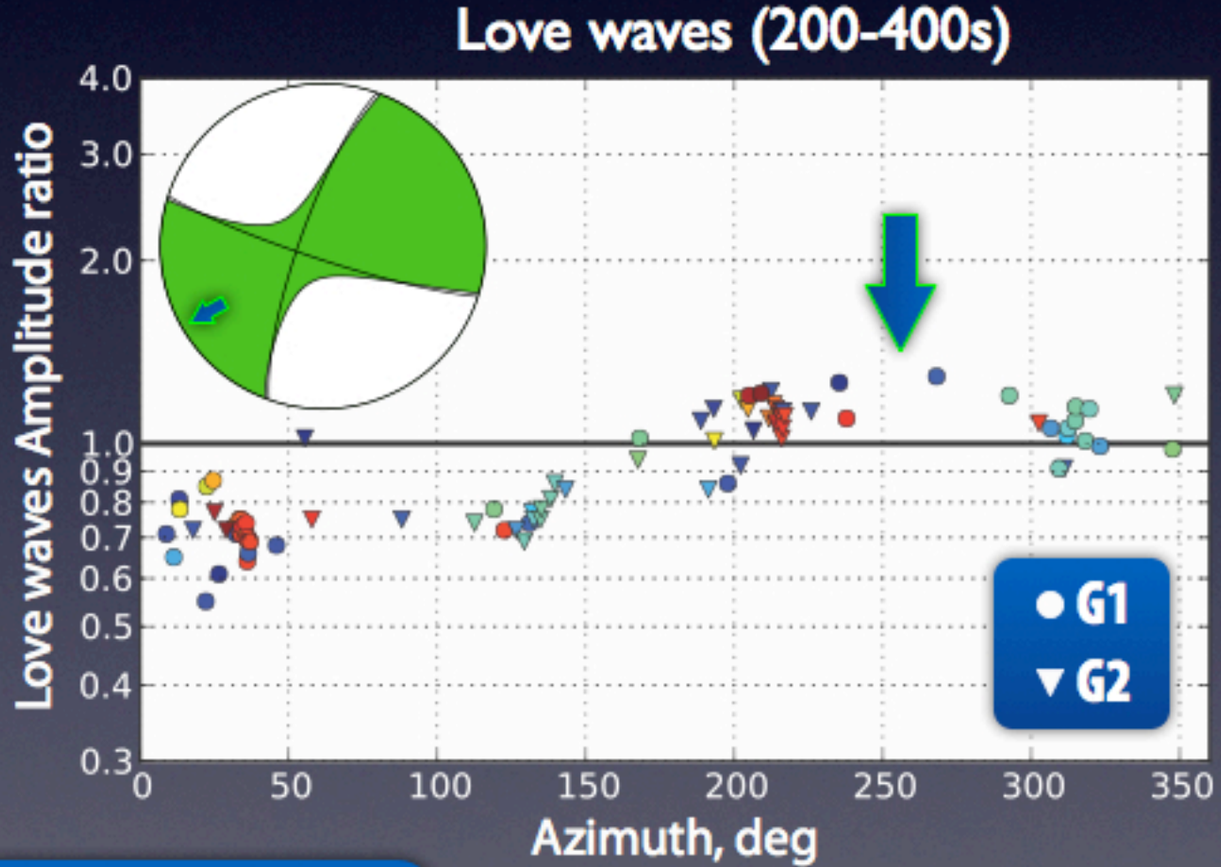

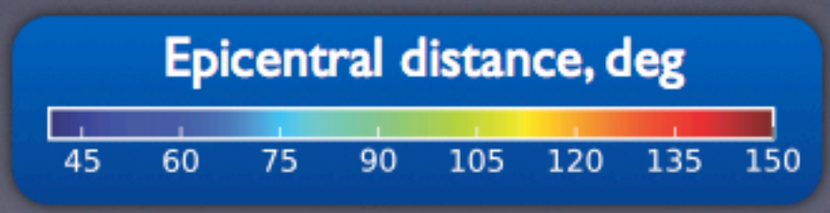

II. Surface-wave directivity for the Mw8.6 mainshock

Surface-wave Moment rate functions (MRF)

- Short-arc Rayleigh-wave (R1), Broad-band (25-600 s)
- Point source SEM synthetics (S362ANI+Crust2.0)
- Projected landweber deconvolution method

Directivity parameter $\Gamma = \cos(\varphi - \varphi_r)/c$

- Allows us to transform any cosine azimuthal moveout into a linear moveout

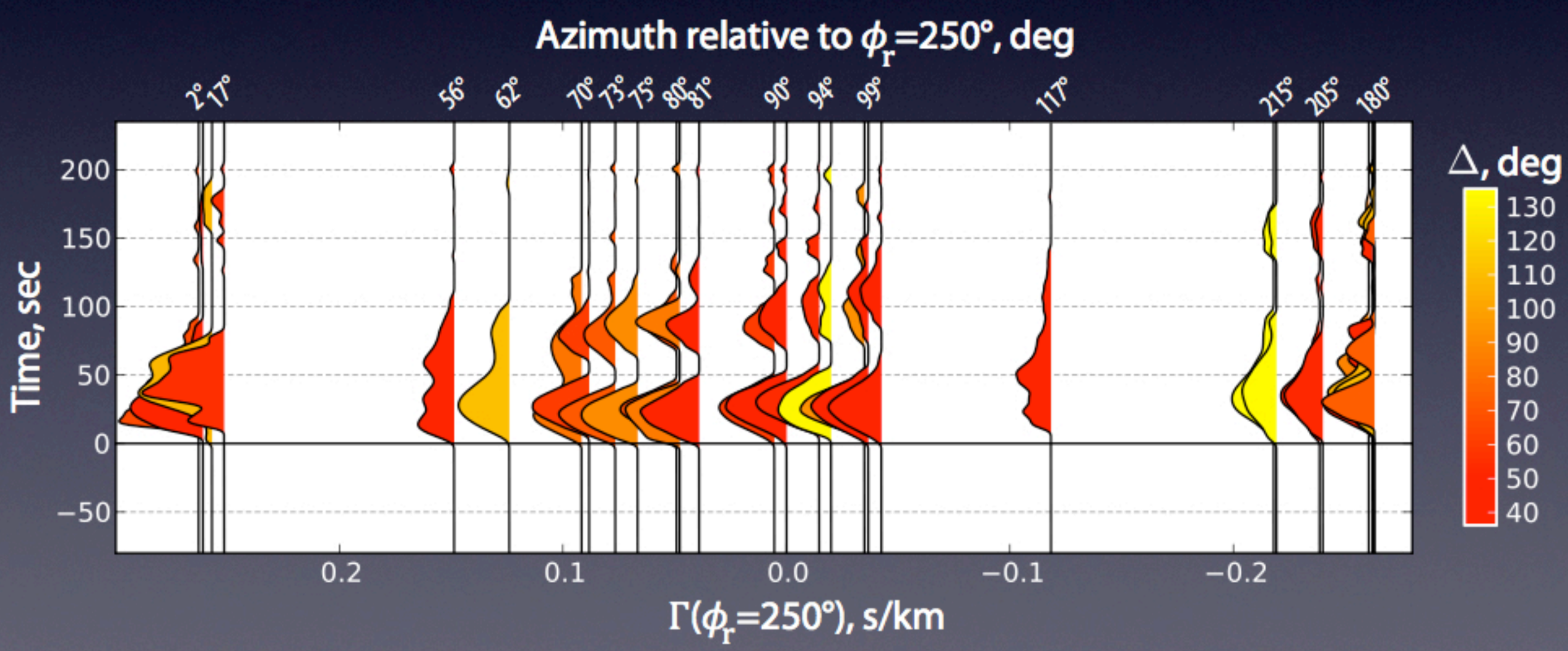

II. Surface-wave directivity for the Mw8.6 mainshock

Directivity effect in the southwest direction also visible here

- Large amplitudes and short duration in the southwest direction
- Duration increases with decreasing directivity parameter

Two distinct pulses

- Second pulse shifts systematically to later times
- Suggests rupture partitioning into at least two distinct subevents.

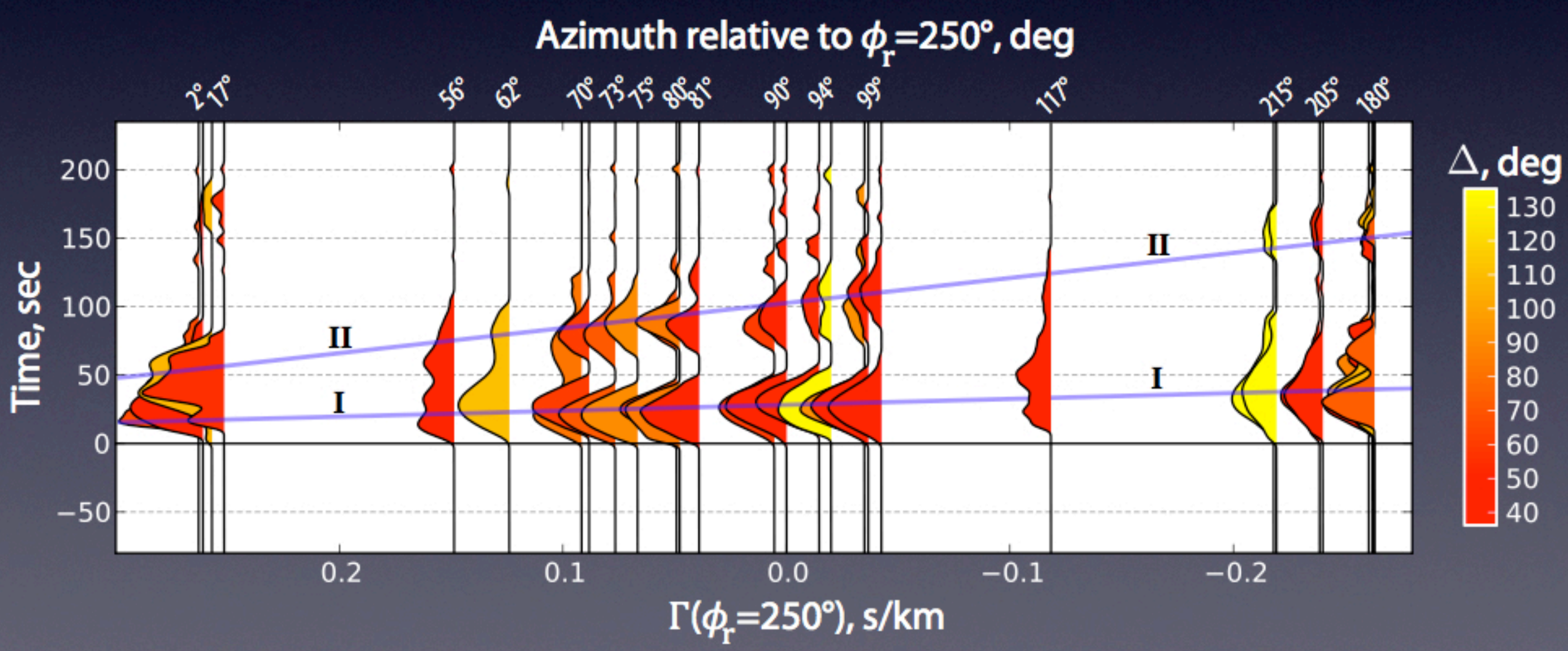

III. Multiple-point-source inversion

Observables:

- W Phase waveforms at shorter period than is typically used for single-point-source inversions of Mw>8.0 events (150-500s).

Parameters:

- Seismic moment tensor: Focal mechanism, Mw
- Point source location
- Timing

Neighbourhood Algorithm sampler (Sambridge, 1999):

- 200 iterations
- 100 samples / iteration
- 50 resampled cells / iteration

Two-point-source inversion: 2012 off-Sumatra mainshock

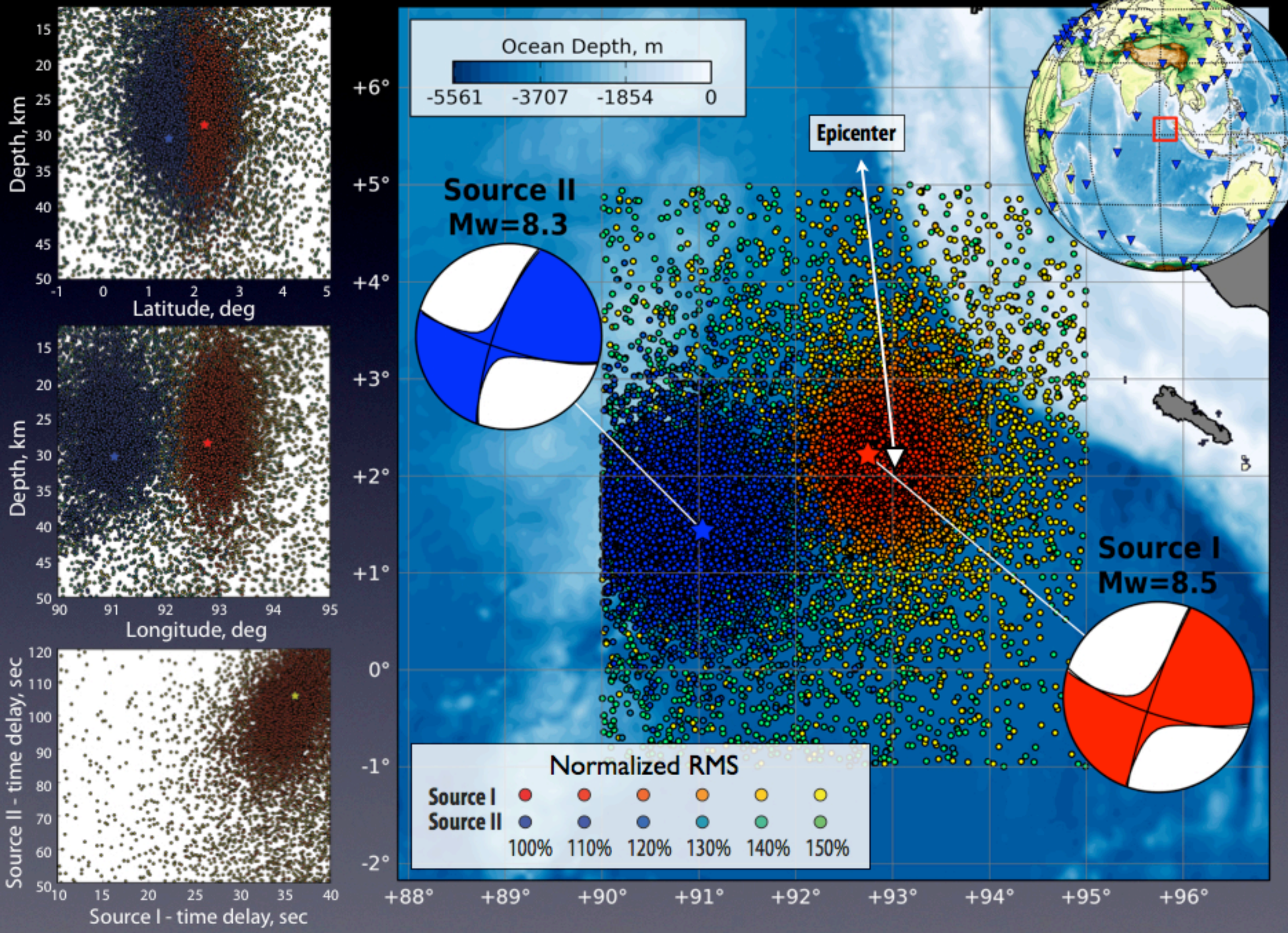

Two-point-source inversion: 2012 off-Sumatra mainshock

BRVK, LHZ

MBAR, LHN

TIXI, LHN

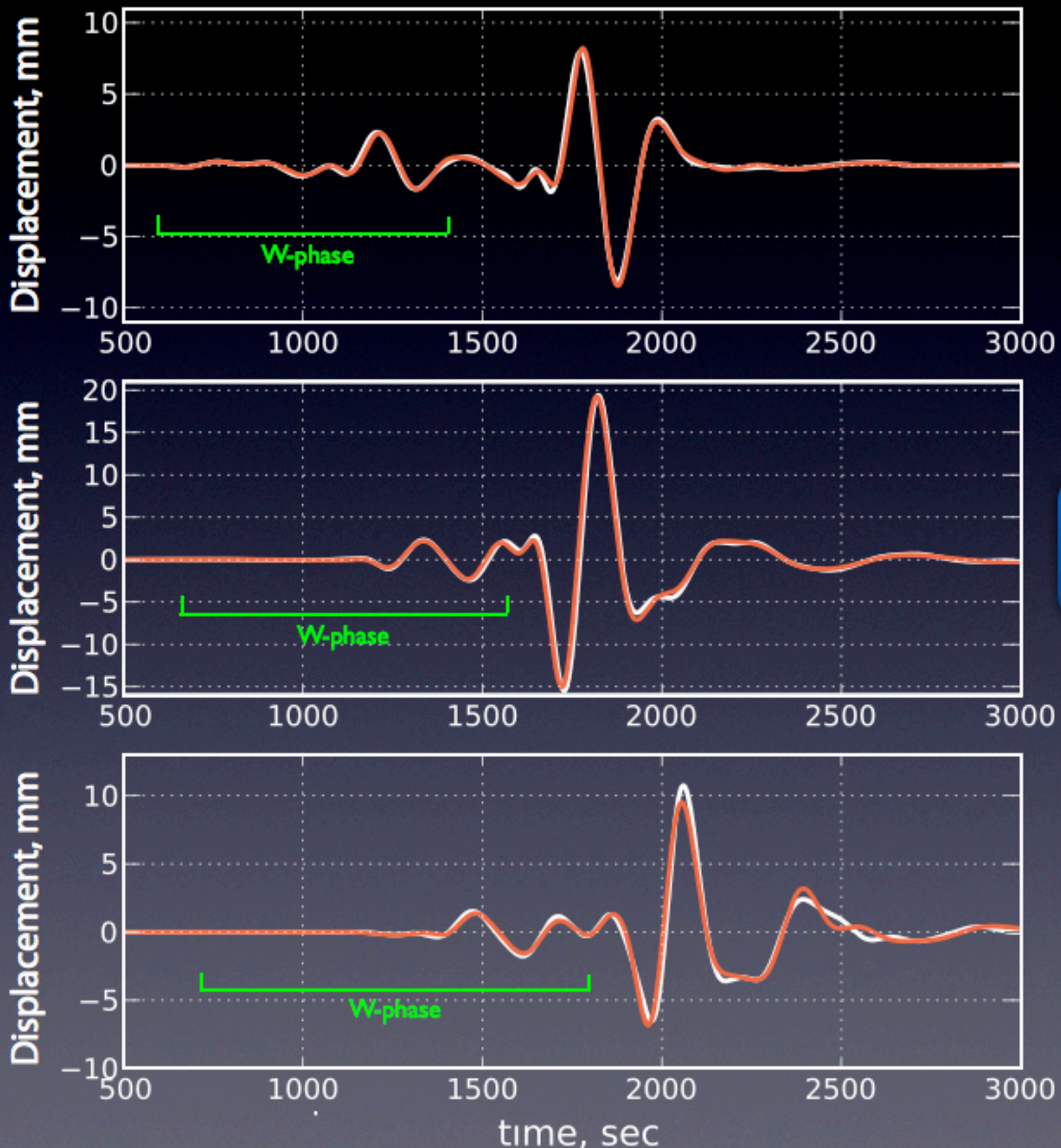

First-order directivity analysis

Observed

Predicted

Rayleigh waves

Love waves

Single-point source

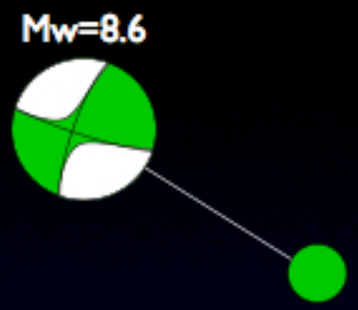

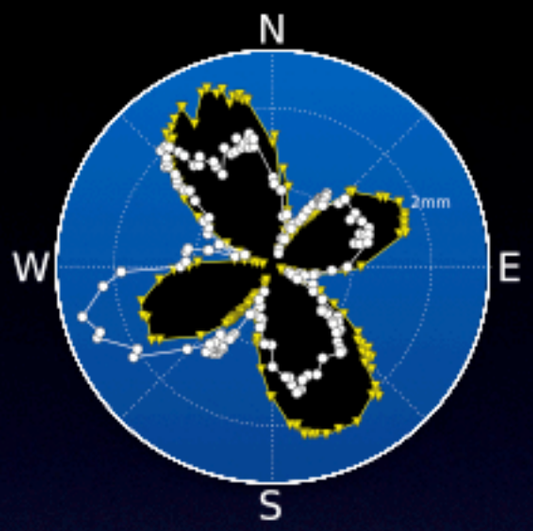

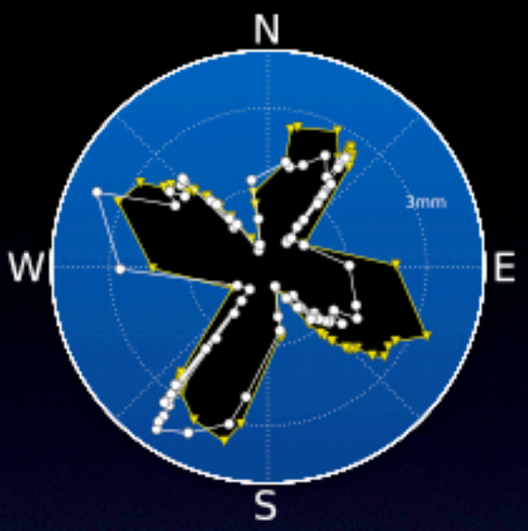

Two-point source

Most robust 0th order model to explain radiation patterns asymetry

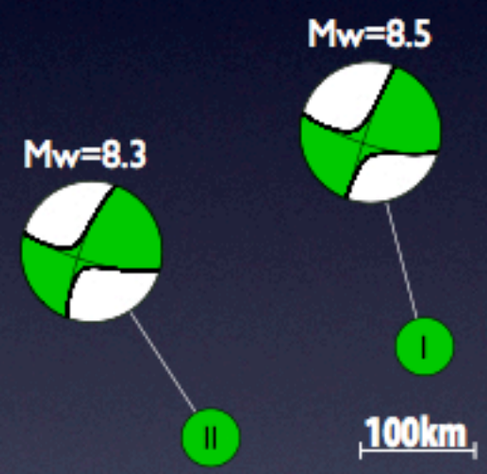

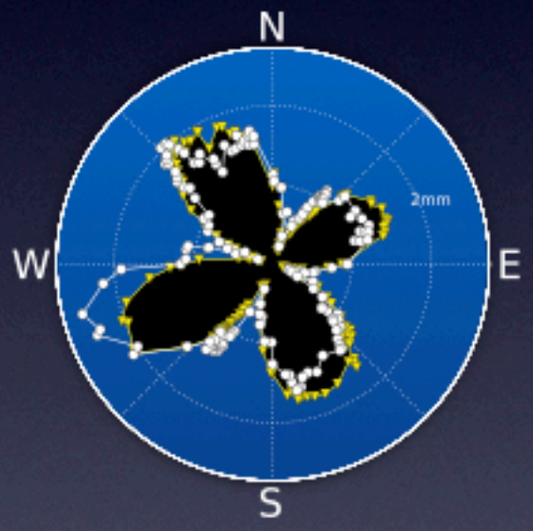

+ Directivity

- Uniform slip distribution
- V_R=1.8km/sec, T_R=25sec
- Parameters: L_1, L_2, Az

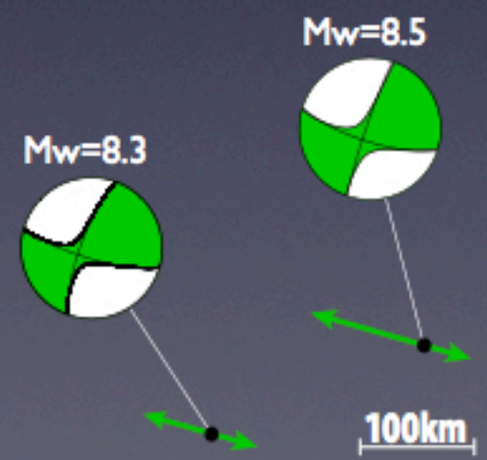

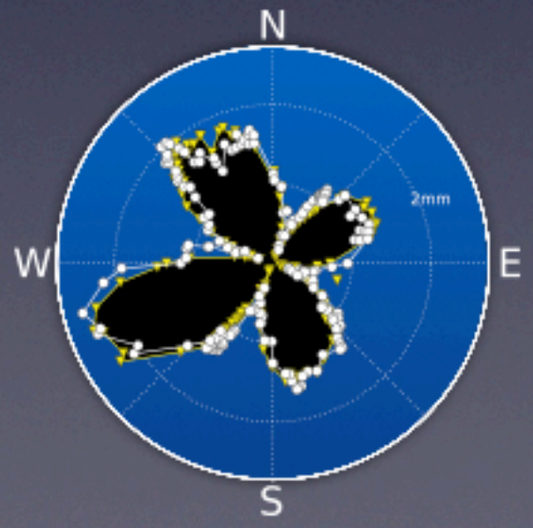

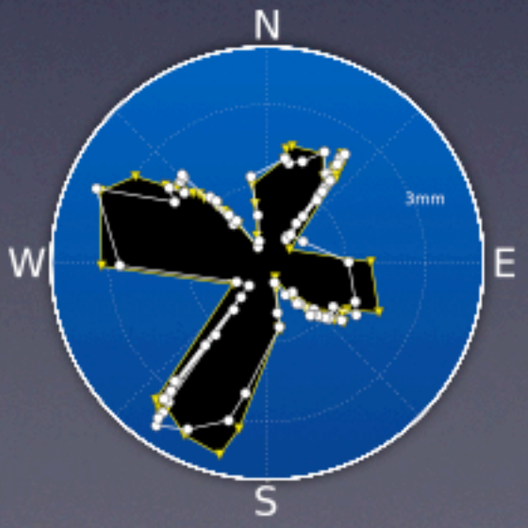

Comparison with preliminary finite-fault models

- Larger contribution from WNW-ESE faults to the total scalar moment

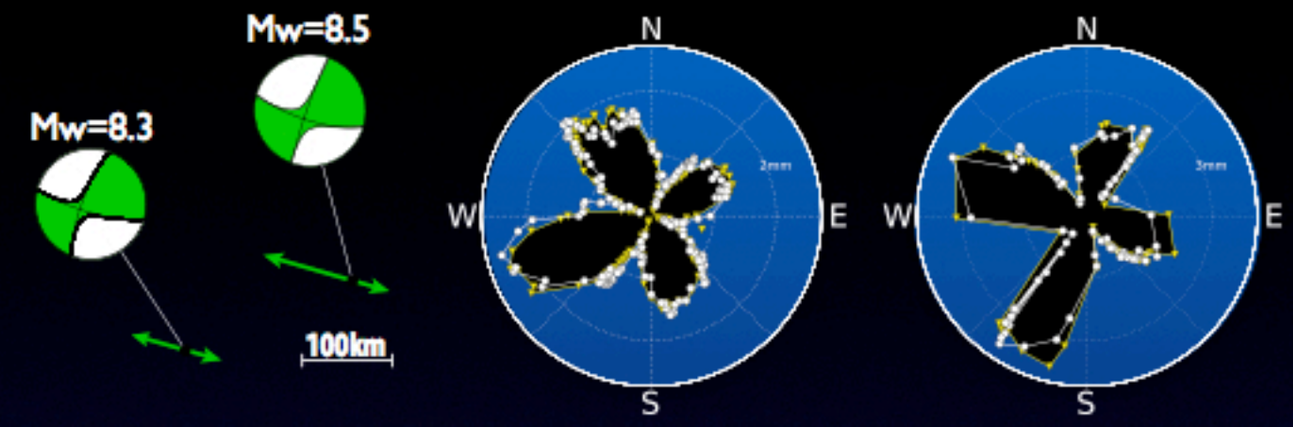

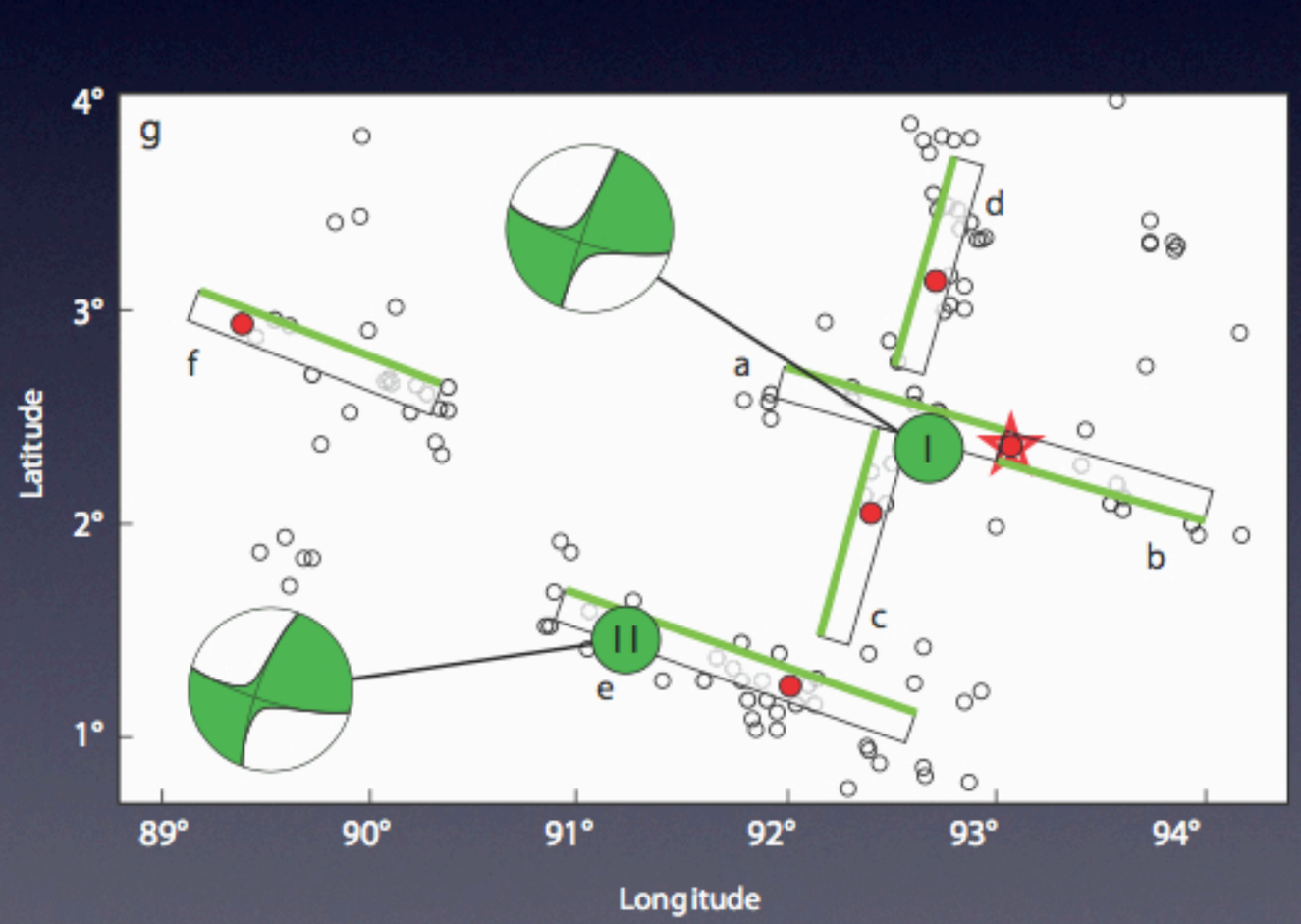

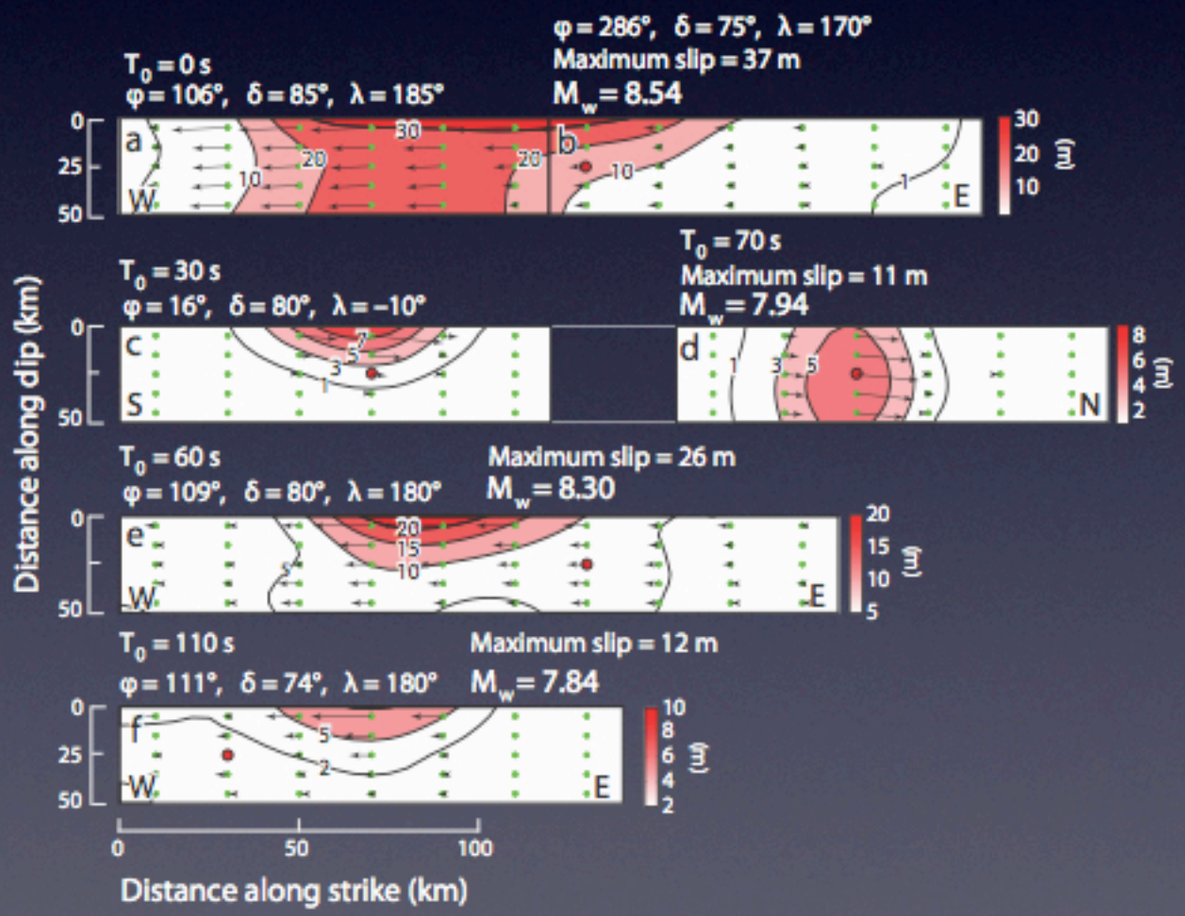

Yue et al. (Nature, 2012)

Comparison with preliminary finite-fault models

- Larger contribution from WNW-ESE faults to the total scalar moment

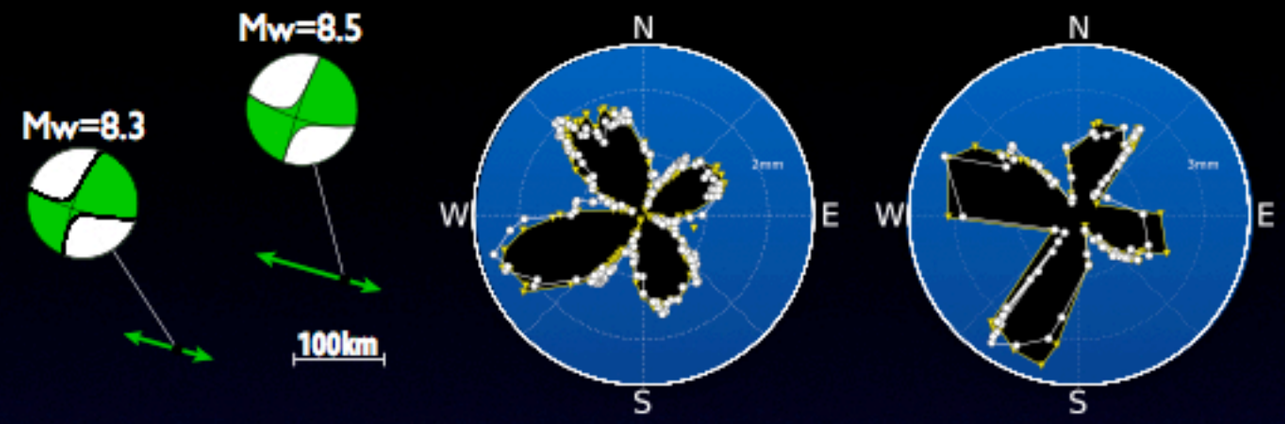

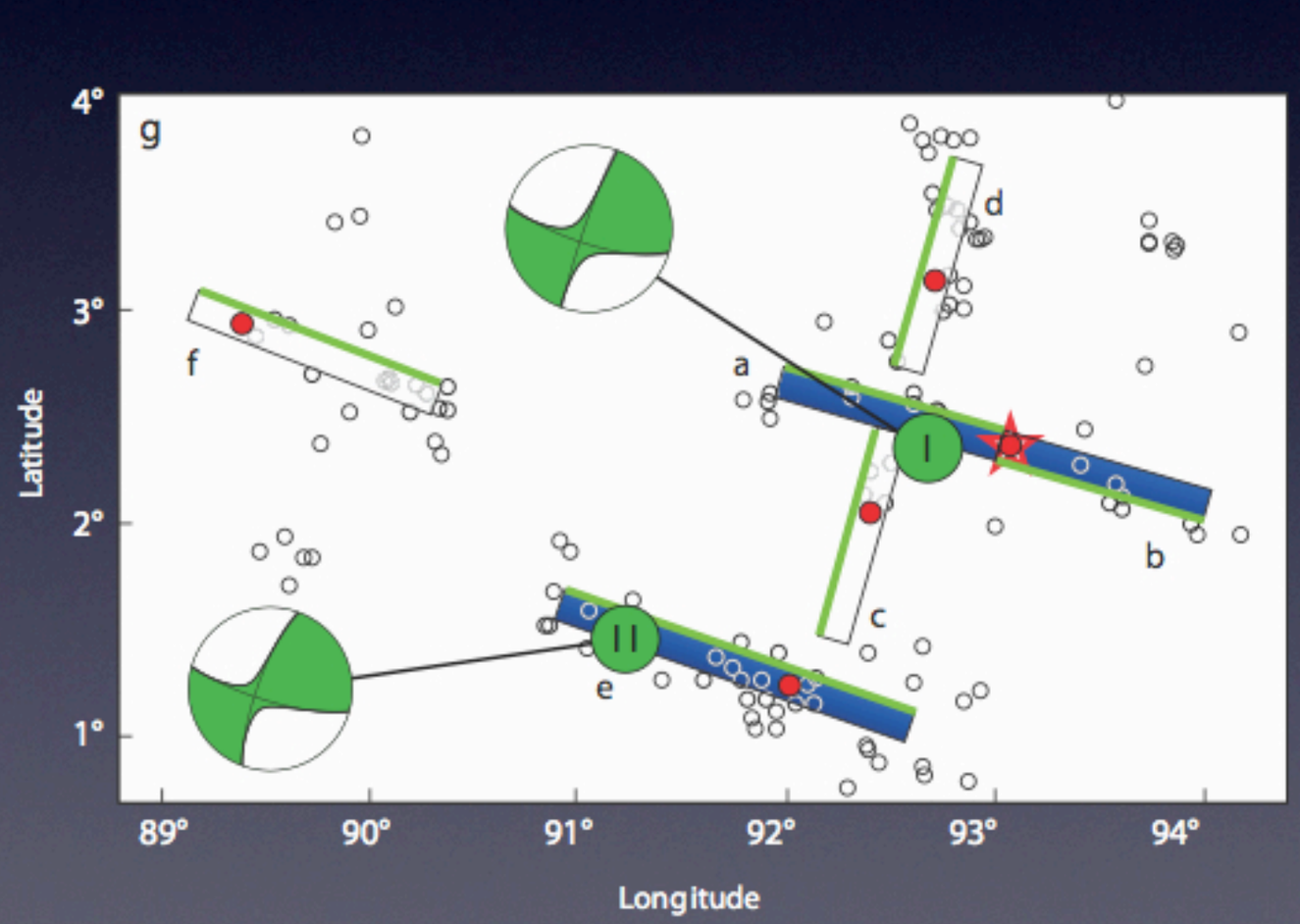

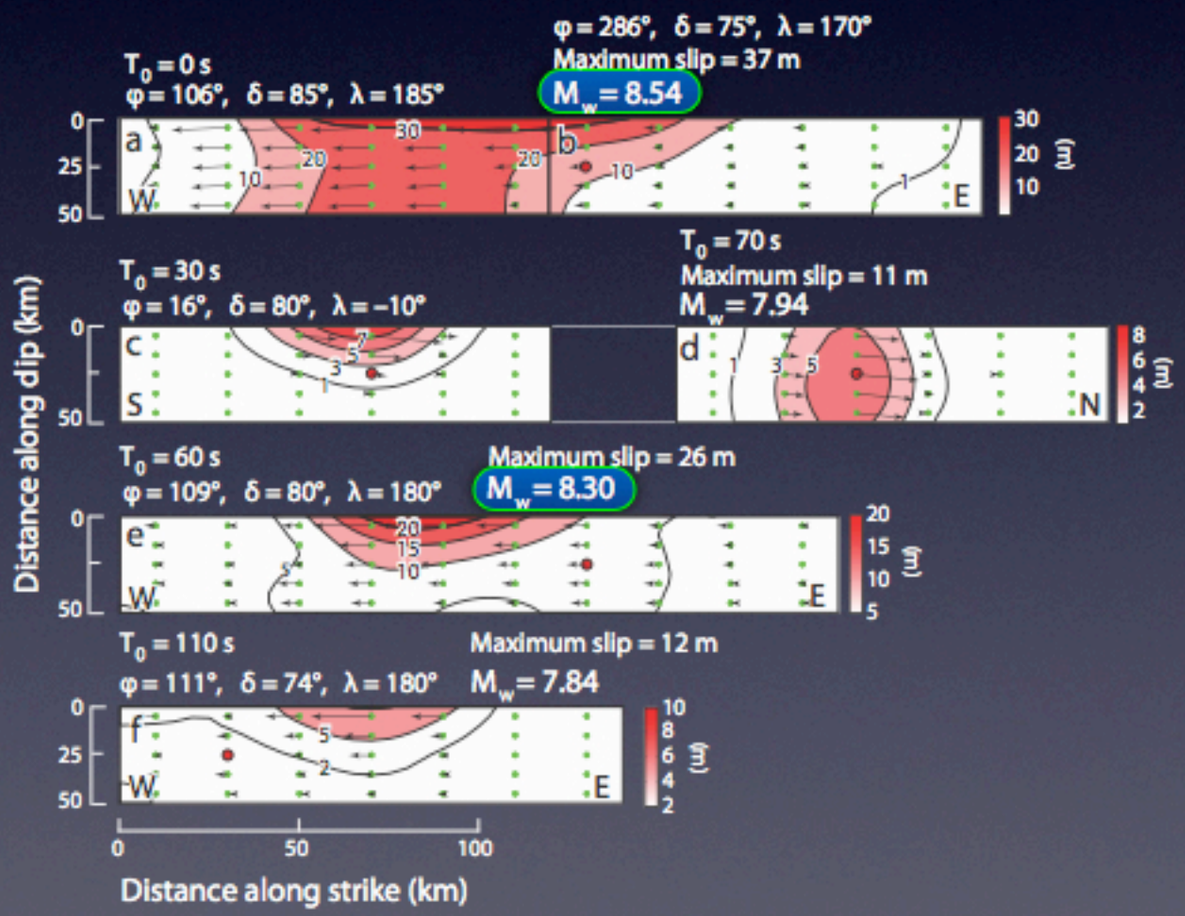

Yue et al. (Nature, 2012)

Centroid Depth: Mw=8.6 Mainshock

- Rayleigh wave amplitude (Love wave amplitude~constant)

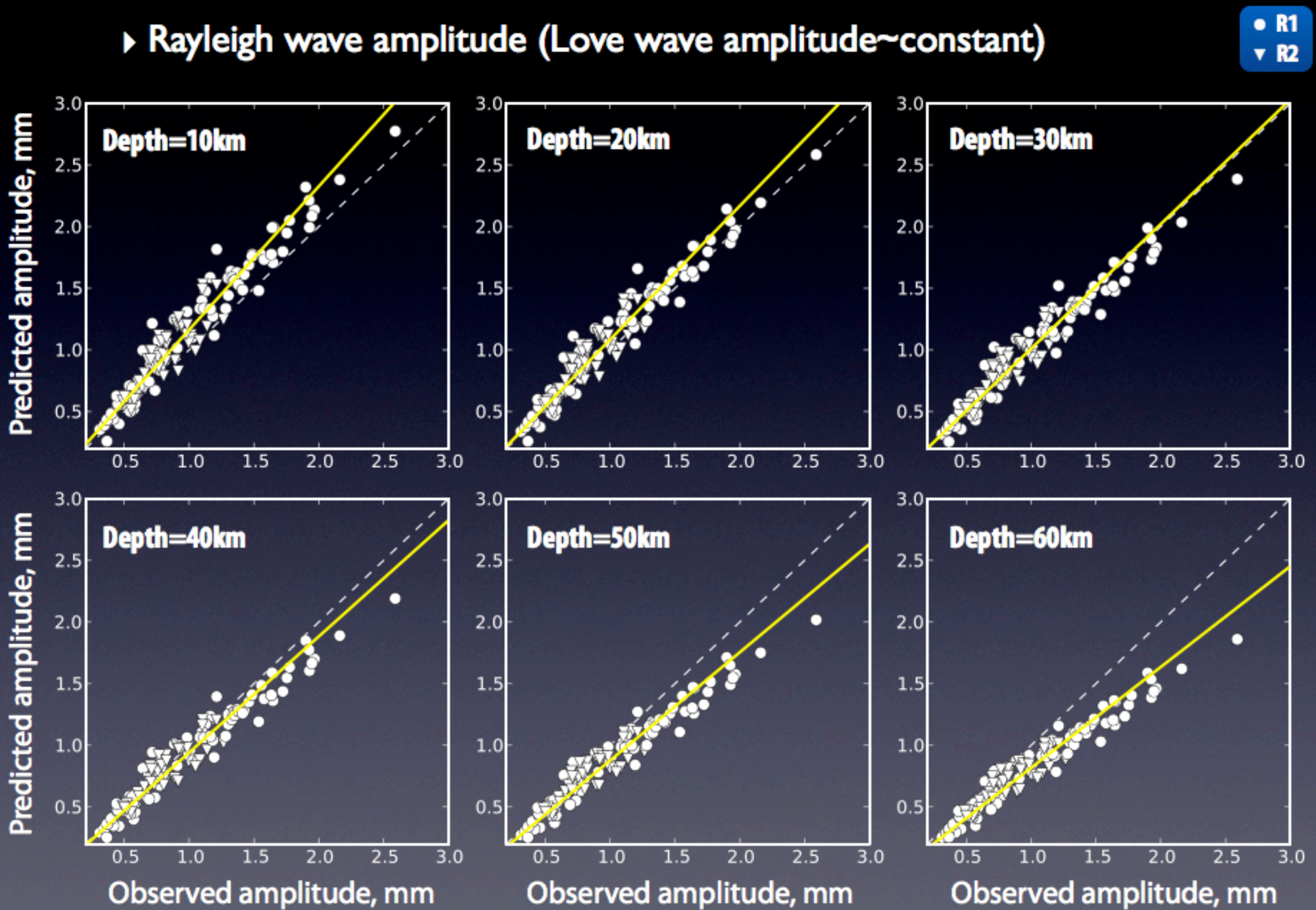

Centroid Depth: Mw=8.2 Aftershock

- Rayleigh wave amplitude (Love wave amplitude~constant)

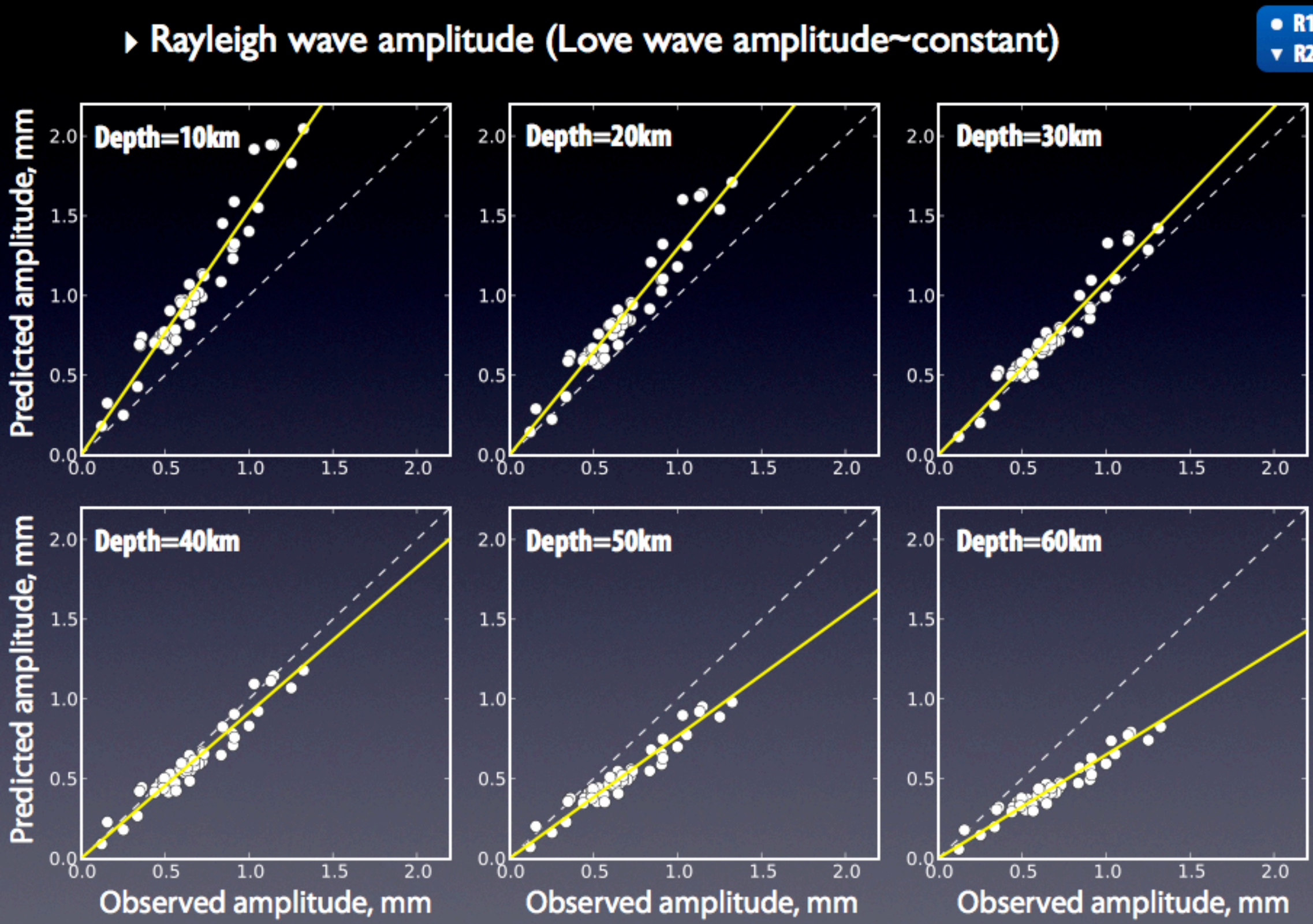

Centroid Depth: Slip distribution for H_C=30km

Hard Numbers:

- Seismic moment: M0=9.2x10^{21}N.m
- Centroid Depth: H_C=30km

The total rupture length L is not well constrained but a reasonnable estimate (from directivity, etc.) is L=200km for which substantial slip occured

- Uniform: $D=M0/[2x\mu xLxH_C]$
- Linear: $D_{(H=0)}=2xM0/[3x\mu xLxH_C]$

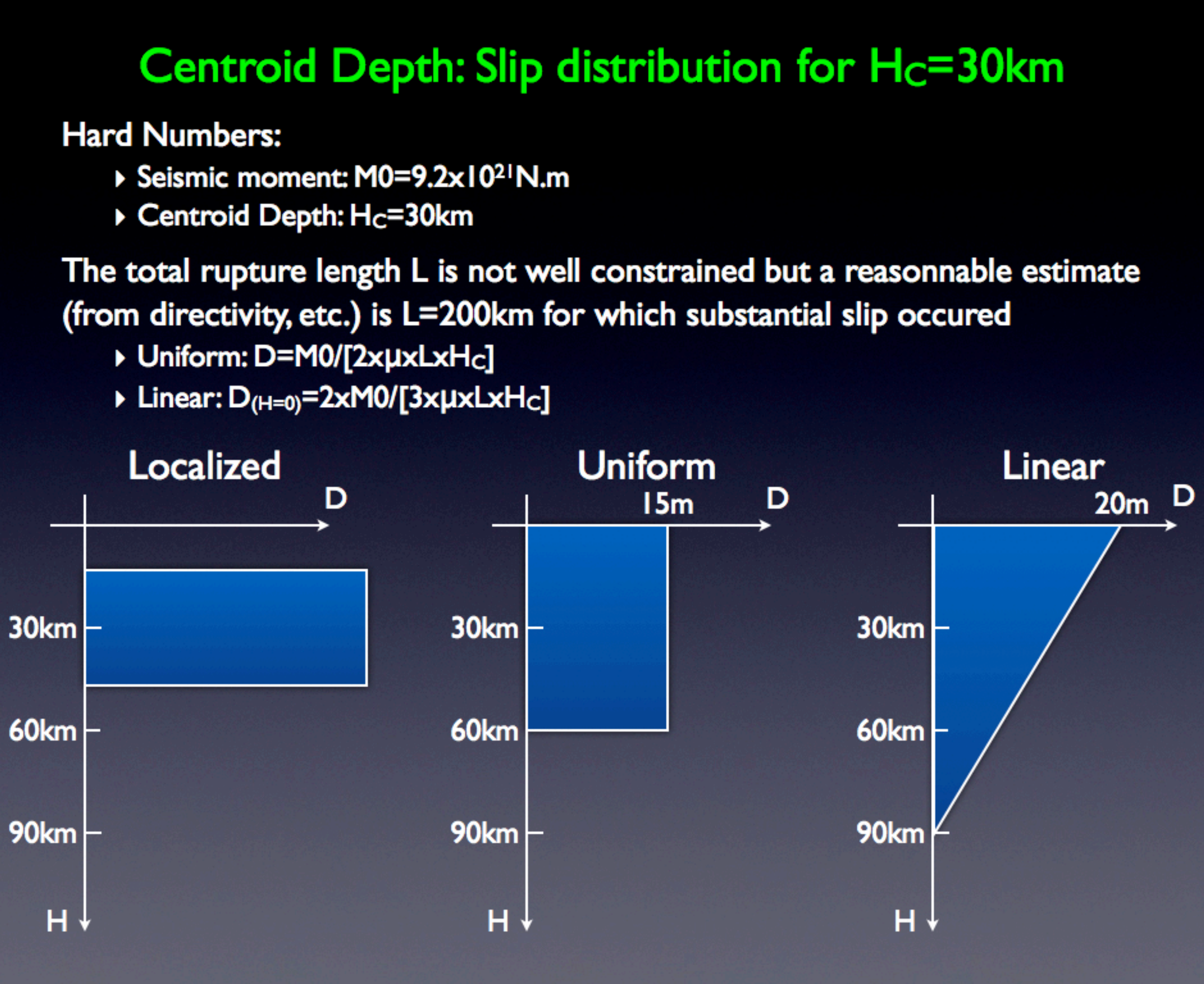

Conclusion

- Various seismological observations reveal a remarkable complexity.

- Our analysis of long-period seismic waves yielded a two-point-source model for the Mw=8.6 mainshock.
  - Source I: Mw=8.5, O.T.+ 36sec
  - Source II: Mw=8.3, O.T.+106sec

- To explain the remaining discrepancy in the radiation patterns, we can invoke a simple WNW-ESE asymmetric bilateral rupture
  - We do not exclude complicated models involving NNE-SSW ruptures as long as they do not violate constraints from long-period seismic waves (i.e., M_0, radiation patern, directivity).

- Large centroid depth both the Mw=8.6 mainshock and the Mw=8.2 aftershock (H_C~30km).
  - Suggests a relatively large depth extent of faulting,
  - Reveals active deep lithospheric deformation.

For more information...

ECGS Workshop:

- Ampuero - Friday afternoon session: *Insights on earthquake dynamics enabled by high-frequency source imaging with dense seismic arrays.*
- Meng et al. - Poster 17: *Compressional rupture branching in a weakened oceanic lithosphere during the 11 April 2012 Mw8.6 Sumatra eartquake.*

2 published articles:

Meng et al. (Science, 2012)

Earthquake in a Maze: Compressional Rupture Branching During the 2012 M_w 8.6 Sumatra Earthquake

L. Meng,* J.-P. Ampuero, J. Stock, Z. Duputel, Y. Luo, V. C. Tsai

Seismological observations of the 2012 moment magnitude 8.6 Sumatra earthquake reveal unprecedented complexity of dynamic rupture. The surprisingly large magnitude results from the combination of deep extent, high stress drop, and rupture of multiple faults. Back-projection source imaging indicates that the rupture occurred on distinct planes in an orthogonal conjugate fault system, with relatively slow rupture speed. The east-southeast–west-northwest ruptures add a new dimension to the seismotectonics of the Wharton Basin, which was previously thought to be controlled by north-south strike-slip faulting. The rupture turned twice into the compressive quadrant, against the preferred branching direction predicted by dynamic Coulomb stress calculations. Orthogonal faulting and compressional branching indicate that rupture was controlled by a pressure-insensitive strength of the deep oceanic lithosphere.

The 11 April 2012 moment magnitude (M_w) 8.6 earthquake off shore of Sumatra is a record-breaking event in many respects. It is the largest strike-slip and intraplate earthquake ever recorded and, as shown here, one of the most complicated ruptures ever imaged by modern seismology. The faulting geometry and spatiotemporal evolution of the main HF sources (Figs. 1 and 2) is remarkably complex. The rupture involved at least three different, almost orthogonal, faults. Their strikes are consistent with the conjugate planes of centroid moment tensor (CMT) solutions and with the distribution of aftershocks (Fig. 1). The rupture process continuity (*8*). Considering uniform slip in a 500-km-long and 40-km-deep rupture, the estimated average slip is ~15 m, and the stress drop is ~15 MPa, which is high but similar to the stress drop of other large oceanic strike-slip earthquakes (*9*, *10*) and not unusual for intraplate and subcrustal earthquakes (*11*, *12*). The multisegment rupture was encouraged by stressing from the M_w 9.1 2004 Sumatra megathrust earthquake, whose southernmost large-slip region coincides with the latitude of the 2012 event (Fig. 1, left). Coulomb stress calculations show that thrust-faulting favors slip on outer-rise strike-slip faults that are oblique to the trench (*13*).

The dominant E-W rupture of faults A, C, and D adds a new dimension to the prevailing view of the seismotectonics of this region. These faults are subparallel to long-lived but still active faults on the NER (Fig. 3) (*14*). The bisecting direction of the conjugate faults is consistent with the orientation of the principal stress inferred from seismic and GPS data (*15*). Strike-slip focal mechanisms from the zone east of the NER have previously been attributed to slip on N-S–striking faults, such as those imaged in seismic lines south of the equator in the Wharton Basin (*16*). Active E-W–striking faults west of the NER are generally attributed to compressional deformation (*8*),

Duputel et al. (EPSL, 2012)

The 2012 Sumatra great earthquake sequence

Zacharie Duputel [a,*], Hiroo Kanamori [a], Victor C. Tsai [a], Luis Rivera [b], Lingsen Meng [a], Jean-Paul Ampuero [a], Joann M. Stock [a]

[a] Seismological Laboratory, California Institute of Technology, 1200 E. California Blvd., Pasadena, CA 91125, USA
[b] IPGS-EOST, CNRS/Université de Strasbourg, UMR 7516, 5 rue René Descartes, 67084 Strasbourg Cedex, France

ARTICLE INFO

Article history:
Accepted 15 July 2012
Editor: P. Shearer

Keywords:
2012 Sumatra earthquake sequence
intraplate earthquakes
earthquake source observations
seismicity and tectonics
surface waves and free oscillations

ABSTRACT

The equatorial Indian Ocean is a well known place of active intraplate deformation defying the conventional view of rigid plates separated by narrow boundaries where deformation is confined. On 11 April 2012, this region was hit in a couple of hours by two of the largest strike-slip earthquakes ever recorded (moment magnitudes Mw=8.6 and 8.2). Broadband seismological observations of the Mw=8.6 mainshock indicate a large centroid depth (~30 km) and remarkable rupture complexity. Detailed study of the surface-wave directivity and moment rate functions clearly indicates the partition of the rupture into at least two distinct subevents. To account for these observations, we developed a procedure to invert for multiple-point-source parameters. The optimum source model at long period consists of two point sources separated by about 209 km with magnitudes Mw=8.5 and 8.3. To explain the remaining discrepancies between predicted and observed surface waves, we can refine this model by adding directivity along the WNW–ESE axis. However, we do not exclude more complicated models. To analyze the Mw=8.2 aftershock, we removed the perturbation due to large surface-wave arrivals of the Mw=8.6 mainshock by subtracting the corresponding synthetics computed for the two-subevent model. Analysis of the surface-wave amplitudes suggests that the Mw=8.2 aftershock had a large centroid depth between 30 km and 40 km. This major earthquake sequence brings a new perspective to the seismotectonics of the equatorial Indian Ocean and reveals active deep lithospheric deformation.

Thanks for your attention